TECHNICAL NOTE
D-611

FAR-FIELD NOISE CHARACTERISTICS

OF SATURN STATIC TESTS

By Wade D. Dorland

George C. Marshall Space Flight Center
Huntsville, Alabama

NATIONAL AERONAUTICS AND SPACE ADMINISTRATION

WASHINGTON

August 1961

NATIONAL AERONAUTICS AND SPACE ADMINISTRATION

TECHNICAL NOTE D-611

FAR-FIELD NOISE CHARACTERISTICS OF SATURN STATIC TESTS

By Wade D. Dorland

SUMMARY

A far-field survey has been conducted to determine the characteristics of the noise generated by the Saturn static firing tests. Data obtained for the first series of eight tests indicate the noise has high power, broad directivity, a low frequency spectrum, and low efficiency. Initial tests were made firing two engines on the first test and four engines on the second test. These tests produced sound power levels of 0.56 megawatt and 1.6 megawatts, respectively, with low efficiencies of 0.04% and 0.06%. The remaining six tests were made with eight engines. They produced sound power levels ranging from 25 megawatts to 40 megawatts, with an acoustic efficiency of approximately 0.7%. Frequency spectra peaked between 10 cps and 100 cps, with a severe dip at 250 cps and a minor peak at 1000 cps. The effects of impingenment on the the flame deflector and the dampening of the cooling water make it very difficult to isolate the effects of clustering the engines.

INTRODUCTION

When the decision was made to conduct static firing tests of the Saturn booster it was foreseen that noise from the firings would present a problem. It was realized that characteristics of the noise would be such that hazardous conditions for both people and property could occur. A reputable acoustic consulting firm Bolt, Beranek, and Newman, Inc., was employed to make a detailed study of the situation. (References 1, 2, and 3). The results of this and later studies confirmed the earlier concern over the possibilities, and emphasized the need for more information on the subject. As a result, an extensive program of noise measurement was established for the Saturn tests. Several interim reports have been written to present initial results of the measurement program. The purpose of this report is to summarize the results and describe the characteristics of the Saturn noise.

UNUSUAL TERMS

SOUND PRESSURE LEVEL - The root-mean-square sound pressure is expressed in decibels. The decibel is $20 \log_{10} \frac{P_1}{P_o}$ where $P_o = 0.0002$ microbar (dyne/sq. cm.).

POWER LEVEL - The acoustic power level is expressed in decibels. In this case, the decibel is $10 \log_{10} \frac{\text{Power}_1}{\text{Power}_o}$ where $\text{Power}_o = 10^{-13}$ watts. Acoustic power is expressed in watts.

SPACE AVERAGE SOUND PRESSURE LEVEL - The sound pressure level in a noise survey averaged over the hemispherical area through which all the acoustical energy radiates.

DIRECTIVITY CORRECTION FACTOR - Shows the difference in the radiation of sound energy through space from a specific noise source to the radiation through space from a sound source with a perfectly spherical radiation.

OCTAVE BAND - A portion of the frequency spectra where the upper limit is double the lower limit.

ONE-THIRD OCTAVE BAND - A frequency bandwidth one-third as wide as an octave band, usually identified by the center frequency of the bandwidth.

NON-STANDARD ABBREVIATIONS

SPL	- Sound Pressure Level
SPL_θ	- Sound Pressure Level at a Station at θ Degrees Angular Coordinate
OA SPL	- Over-all Sound Pressure Level
PWL	- Power Level
$\overline{SPL}_H$	- Space Average Sound Pressure Level
OB	- Octave Band

1/3 OB - One-Third Octave Band

OBL - Sound Pressure Level in an Octave Band

1/3 OBL - Sound Pressure Level in a One-Third Octave Band

LOCATIONS OF INSTRUMENTS

From a source located in space, and assuming that still air is the transferring medium, sound is radiated uniformly in all directions. The sound energy is dispersed through the surrounding sphere and the intensity decreases inversely as the square of the distance from the source. The ideal sound measuring system would then have instruments located on the surface of a hypothetical sphere of some known radius. For a sound source located at or near ground level, the hypothetical sphere is reduced to a hemisphere. And for a hemisphere with an appreciable radius, it is feasible to have instruments placed only on a circle at ground level where the hemisphere would touch the earth. Since instrumentation channels were limited in number and under the assumption that radiation of energy would be uniform to both sides, the instruments for the Saturn program were placed on a semicircle. Figures 1 and 2 show the test position, and Figure 3 shows a plan view of the test position and the layout of instrumentation. It will be noted that along the 60^{o} angular coordinate, instruments were placed at distances which are successively doubled. This was done to check the inverse square law of radiation intensity. Details of the measuring system and its calibration, and of the system used for data reduction are presented in Appendix A and on Figure 29.

RESULTS

Sound measurements have been made for all Saturn tests to date. Data secured show that the characteristics of the noise for the two-engine and the four-engine tests are quite different from those for the eight-engine tests. This can be attributed to three factors. The first, and perhaps most important factor, is that such differences are a result of the various cluster combinations. This was foreseen and expected. A second reason for such differences is that extensive modifications in the flame deflector were made concurrently with the first tests. The changes included a slotted extension and a secondary, flat-plate deflector. No doubt, both had considerable effect on directivity and frequency. The deflector modifications are outlined in Figure 4. A third factor is that, during the development of the deflector, the

coolant water flowrate was changed from test to test. This resulted in a varied sound dampening effect and a corresponding change in noise characteristics. The individual effects of these factors cannot be isolated and it can only be pointed out that the changes in noise characteristics shown are a result of all three.

Recorded data for the first eight tests are plotted to give the sound spectra shown on Figures 5 to 17. Data for the two-engine, four-engine, and first eight-engine tests are plotted separately. Data for the last five eight-engine tests are averaged for conciseness. The main body of each graph presents the characteristics for each group at specific frequencies. The extreme left end of each graph shows the overall sound level for each group, and the overall sound level range for the last five eight-engine tests.

Figures 18 to 23 are graphs of the possible amplitude distributions indicated by recorded data. A thorough and detailed analysis of wave form has not yet been made. A normal (Gaussian) distribution curve with the same area has been plotted for comparison.

From the measured sound pressure levels, the descriptive parameter of directivity has been computed (See Appendix B). Individual sound pressure measurements were averaged over that portion of the theoretical hemisphere used for this survey. This averaged value is termed the Space Average Sound Pressure Level ($\overline{SPL}_H$) and corresponds to the value that would have been measured at each position from a similar sound source radiating in space through a hemisphere. This average value is then compared with the sound pressure level measured at each station (SPL_θ) to give a directivity factor. Results are presented in graphical form on Figures 24 to 26.

An important result of the survey is a descriptive power spectrum for the Saturn jet as a sound source. This has been computed from the space average sound pressure level. Assumptions were that the sound waves lose no energy in the air and that power radiation follows the inverse square law. To facilitate this computation, the 600-foot radius was chosen for locating microphones. This gave at least five full wave lengths for sound frequencies above 10 cps. No doubt there was some attenuation of high frequencies, but it is believed that the assumptions and chosen distances were a sound compromise and gave reasonably valid results. The plotted power spectra are shown on Figures 27 and 28. Tables I and II give details of the test conditions and specific results of the power computations. Table II shows that attenuation was high for the first three tests, resulting in low efficiencies for those tests. Studies based on theory alone indicated that the Saturn booster as a noise source would have an efficiency of about 1.0%. Measured values show an efficiency of about 0.7%.

EVALUATION OF RESULTS

In reviewing the results of this survey, it is believed that the rms sound pressure levels recorded give good indications of the existing rms environments. To fully evaluate the results, consideration must be given to the random characteristics of the noise in question. To facilitate this consideration, the amplitude distribution plots shown on Figures 18 to 23 are presented. The plots show minor deviations from Gaussian randomness and indicate a negative probability of wave form. This may be a result of finite amplitude limiting of air.

Some doubt may arise over the presumption that Saturn noise is attenuated in accordance with the inverse square law of radiation. However, recorded data show a reasonable balance between too much attenuation for some frequencies and too little for others. Therefore, it is considered that such a presumption is valid, within feasibility, and in accordance with established practice for making far-field noise surveys.

The overall directivity is influenced most by the directivity of frequencies below 50 cps. A review of the directivity plots on Figures 27 and 28 indicates this is to be expected, since spectral peaks occur in the lower range. Further inspection of the plots shows directivity of the two-engine and the four-engine tests to be much narrower than for the eight-engine tests. With few exceptions, the lobes of most intense radiation peak at angular coordinates near 50°. For coordinates greater than 50°, the directivity is quite similar for all clusters. Below that value, considerable difference exists in directivity. Modifications to the deflector included an extension which changed the exhaust gas flow from 5° above horizontal to 30° above horizontal. This and other deflector changes doubtless had considerable influence on overall directivity. However, concurrently with deflector changes, the number of engines in use was increased. Different levels of exhaust impingement and resulting interference of individual jets make it impossible to delineate the specific sound source-to-receiver geometry so changes in directivity can only be considered as resulting from both these factors.

Inspection of the pressure spectra plots shown on Figures 24 to 26 reveals severe dips and peaks in some curves, with less severe changes in the slopes of all curves. Jet noise spectra are usually rather smooth and are similar to the spectrum shown on Figure 15. Here again, the exact cause for each deviation is difficult to isolate and can only be attributed to the combination of changes in deflector configuration and number of engines. A survey of noise generated during launch of a Saturn flight vehicle may serve to isolate the respective effects of the factors mentioned.

Referring again to the pressure spectra plots, attention is directed to the width of the curve peaks. These spectra, and the power spectra based on them, were expected to have broad peaks, four to five octaves wide at 8 to 100 cps. (See Reference 1 or 4). Generally, the peaks were about three octaves wide and, for angular coordinates below 30°, were centered near 20 cps. Between 50° and 70°, the peaks were only about two octaves wide and were centered between 40 cps and 60 cps. In the 90° to 150° arc, the peaks were again about three octaves wide, but centered near 80 to 100 cps. Computed power spectra peaks were about four octaves wide, thus averaging out the shifts in spectral peaks found in the pressure spectra.

The small peaks at 2.5 cps are attributed to tape recorder "wow" and should be disregarded. Spectral values above 5000 cps are believed to be slightly high due to internal system noise.

An important characteristic of any noise is the efficiency of the generating source. However, recorded data show an efficiency of about 0.7% for the eight-engine tests and considerably less for the two-engine and the four-engine tests. This is attributed to the following:

(1) The jets merge and create less turbulence than would a single smooth jet with the same kinetic energy.

(2) The length of the central core terminates abruptly at impingement with the deflector, greatly reducing the volume of supersonic flow. This varies from jet to jet as the location of impingement varies.

(3) Considerable dampening results from the large volume of coolant water pumped through the deflector surface. This appears to have had particular effect on the two-engine and four-engine tests where the coolant water flowrate was two or three times the propellant flowrate.

Here again, it is impossible to isolate the individual effects of the three factors and further clarification will be dependent on launch test noise surveys. Although this noise survey was conducted during tests of a prototype research and development vehicle, results are considered valid and may be extrapolated to predict noise characteristics of flight vehicles. Increase of booster thrust to 1,500,000 pounds will probably raise the noise power level about one decibel.

CONCLUSIONS

From the evaluation of the results of this program it has been concluded that:

(1) Not only was a complete description of Saturn eight-engine noise obtained, but fairly complete descriptions were obtained for two-engine and four-engine clusters.

(2) Acoustic powers generated by the cluster configurations are 0.56 megawatt for two engines, 1.6 megawatts for four engines, and 25 to 40 megawatts for eight engines.

(3) The acoustic efficiency is quite low; 0.03% for two engines, 0.06% for four engines, and 0.7% for eight engines.

(4) Sound pressure spectra peak between 10 and 100 cps and are not as smooth as those for single jet engines.

(5) Directivity is fairly narrow for two-engine and four-engine tests, but quite broad for eight engines.

(6) Indications are that clustering jet exhausts results in peaked pressure spectra and low efficiency; however, data obtained so far are insufficient to isolate this effect.

(7) Flight vehicles with a thrust of 1,500,000 pounds are expected to develop about 10% more acoustic power than the research and development vehicle used during this survey.

(8) Results of the noise surveys made at the launch site may make it possible to isolate individual effects of clustering engines, deflector configuration, and dampening effect of coolant water.

TABLE I

SATURN BOOSTER STATIC TEST CONDITIONS

TEST	DATE (1960)	TIME	DURATION (sec)	NO. OF ENGINES	THRUST (lb) *	WATERFLOW (gal/min)	OA $\overline{SPL}_H$ (db) **	OA PWL (dbp)	EFFI-CIENCY (%)	WATER TO PROPELLANT MASS FLOW RATIO *
SA-T-01	March 28	11:00 a.m.	8	2	300K	30,400	124	187½	0.04	3.5
SA-T-02	April 6	11:14 a.m.	6½	4	600K	36,500	128½	192	0.06	2.0
SA-T-03	April 29	5:29 p.m.	8	8	1300K	40,400	137½	201	0.3	1.1
SA-T-04	May 17	5:33 p.m.	24	8	1300K	NA	142½	206	0.8	---
SA-T-05	May 26	5:05 p.m.	35	8	1300K	38,100	142	205½	0.7	1.0
SA-T-06	June 3	5:00 p.m.	75	8	1300K	38,650	142½	206	0.7	1.0
SA-T-07	June 8	4:55 p.m.	110	8	1300K	39,950	139½	203	0.4	1.0
SA-T-08	June 15	5:33 p.m.	121	8	1300K	42,750	140½	204	0.5	1.1

* Nominal Values

** At 600 foot radius

TABLE II

PARTIAL WEATHER CONDITIONS DATA AND INVERSE SQUARE
LAW SOUND PROPAGATION DURING STATIC TESTS OF SATURN BOOSTER

TEST	AIR TEMP-ERATURE (°F)	SURFACE WIND		DISTANCE (ft)	DECREASE IN SPL IN DECADES OF FREQUENCY			IDEAL INVERSE SQUARE LAW PROPAGATION (db)
		DIREC-TION	SPEED (mph)		16 to 100 cps (db)	100 to 1,000 cps (db)	1,000 to 8,000 cps (db)	
SA-T-01	60	SSE	10	150-300	12.5	19.5	18.5	6
				300-600	4.0	7.5	---	6
				600-1200	9.5	11.5	---	6
SA-T-02	62	SSW	18	150-300	6.5	11.5	11.0	6
				300-600	2.5	6.5	6.5	6
				600-1200	6.0	9.0	8.0	6
SA-T-03	77	S	10	150-300	3.0	8.0	9.5	6
				300-600	6.5	12.0	10.5	6
				600-1200	0.5	8.5	7.0	6
SA-T-04	84	WSW	8	Data not available for estimate on this test				
SA-T-05	74	SE	8	150-300	3.0	8.0	10.0	6
				300-600	0.5	6.0	4.5	6
				600-1200	4.0	9.5	13.2	6

TABLE II (Continued)

TEST	AIR TEMP-ERATURE (°F)	SURFACE WIND		DISTANCE (ft)	DECREASE IN SPL IN DECADES OF FREQUENCY			IDEAL INVERSE SQUARE LAW PROPAGATION (db)
		DIREC-TION	SPEED (mph)		16 to 100 cps (db)	100 to 1,000 cps (db)	1,000 to 8,000 cps (db)	
SA-T-06	75	S	2	150-300 300-600 600-1200	4.0 1.0 3.5	9.5 5.5 8.5	12.0 5.0 5.0	6 6 6
SA-T-07	85	NNW	8	150-300 300-600 600-1200	5.5 5.5 13.5	11.5 11.5 9.5	13.5 8.5 ---	6 6 6
SA-T-08	87	E	4	150-300 300-600 600-1200	1.0 3.5 4.5	7.0 9.5 9.0	9.0 8.5 7.0	6 6 6

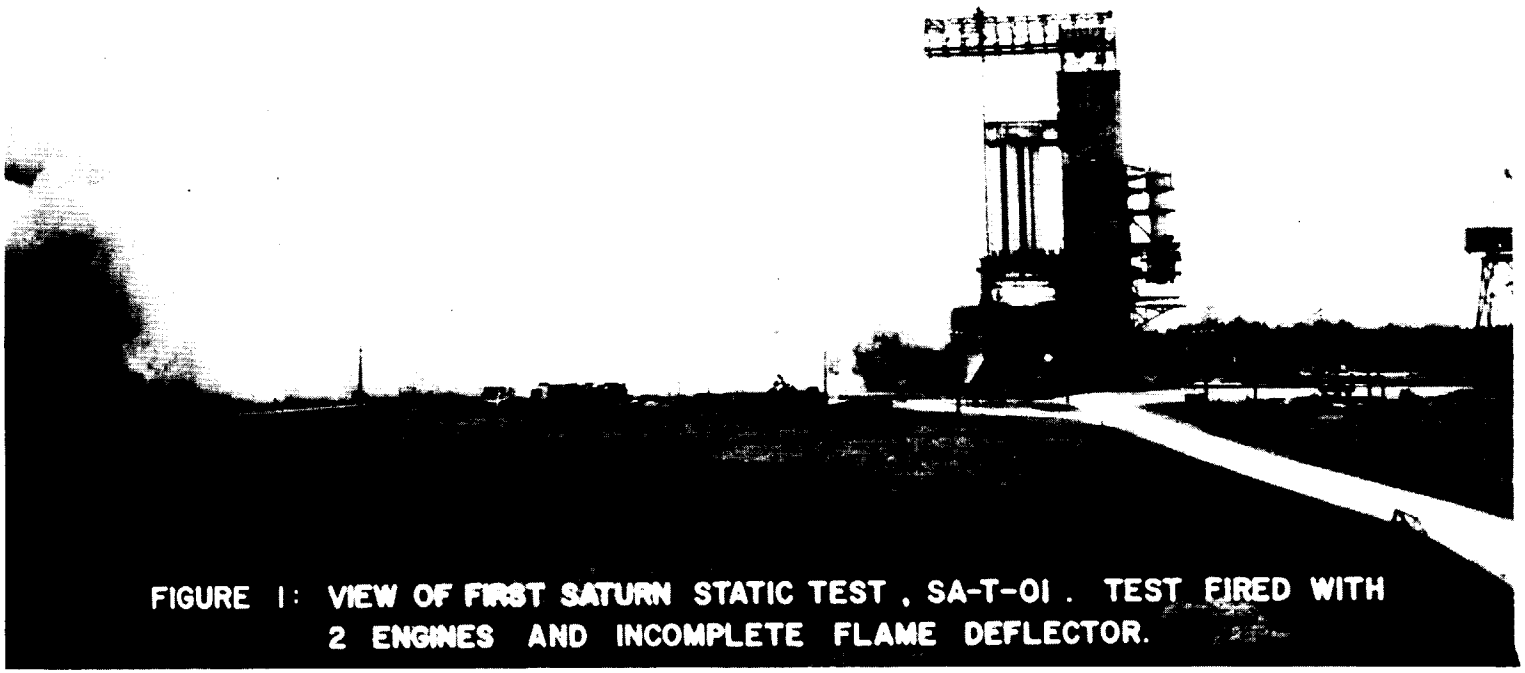

FIGURE 1: VIEW OF FIRST SATURN STATIC TEST, SA-T-01. TEST FIRED WITH 2 ENGINES AND INCOMPLETE FLAME DEFLECTOR.

FIGURE 2: A SATURN STATIC TEST FIRED WITH EIGHT ENGINES AND COMPLETED FLAME DEFLECTOR.

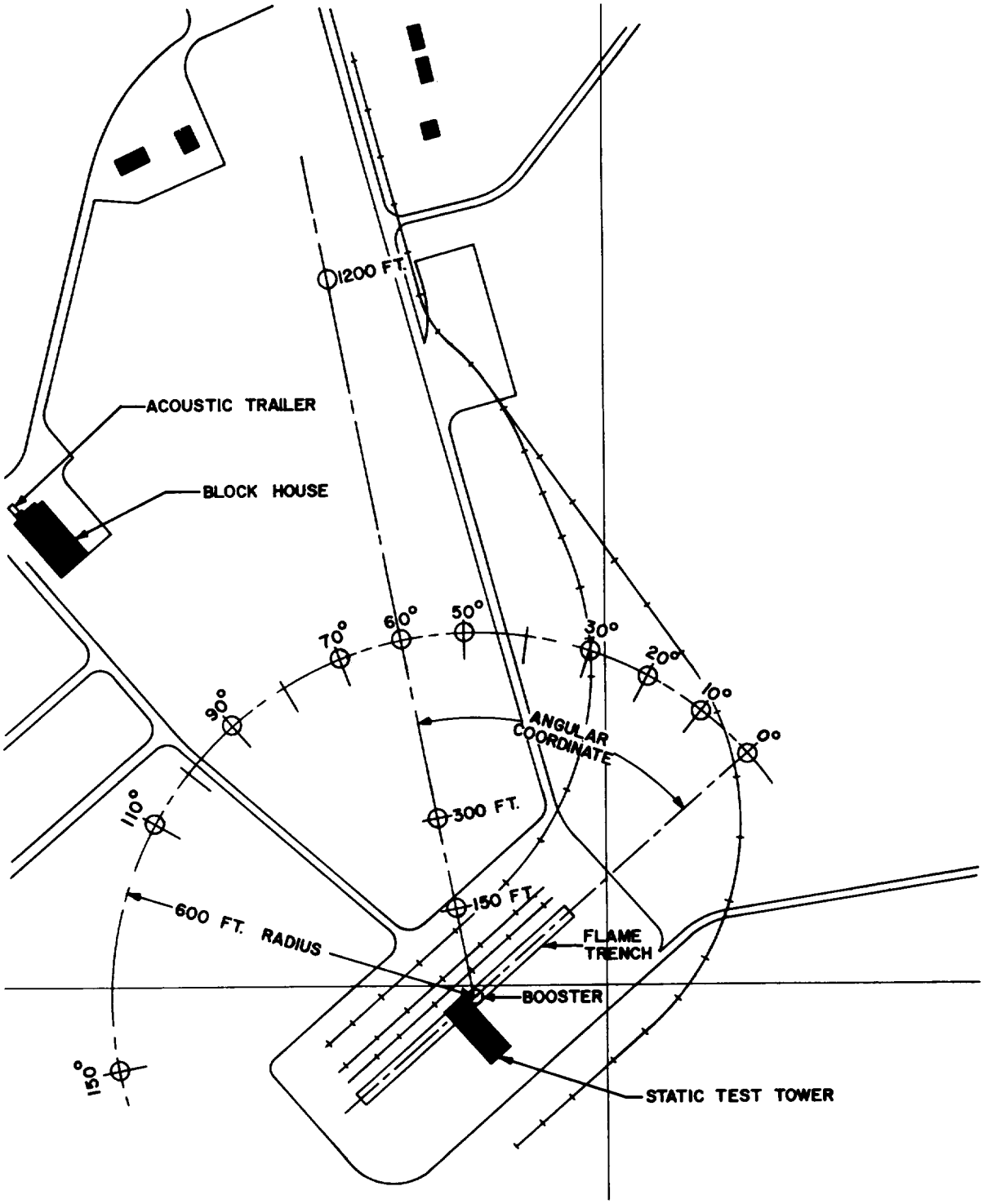

FIGURE 3 – PLAN VIEW OF MICROPHONE ARRAY

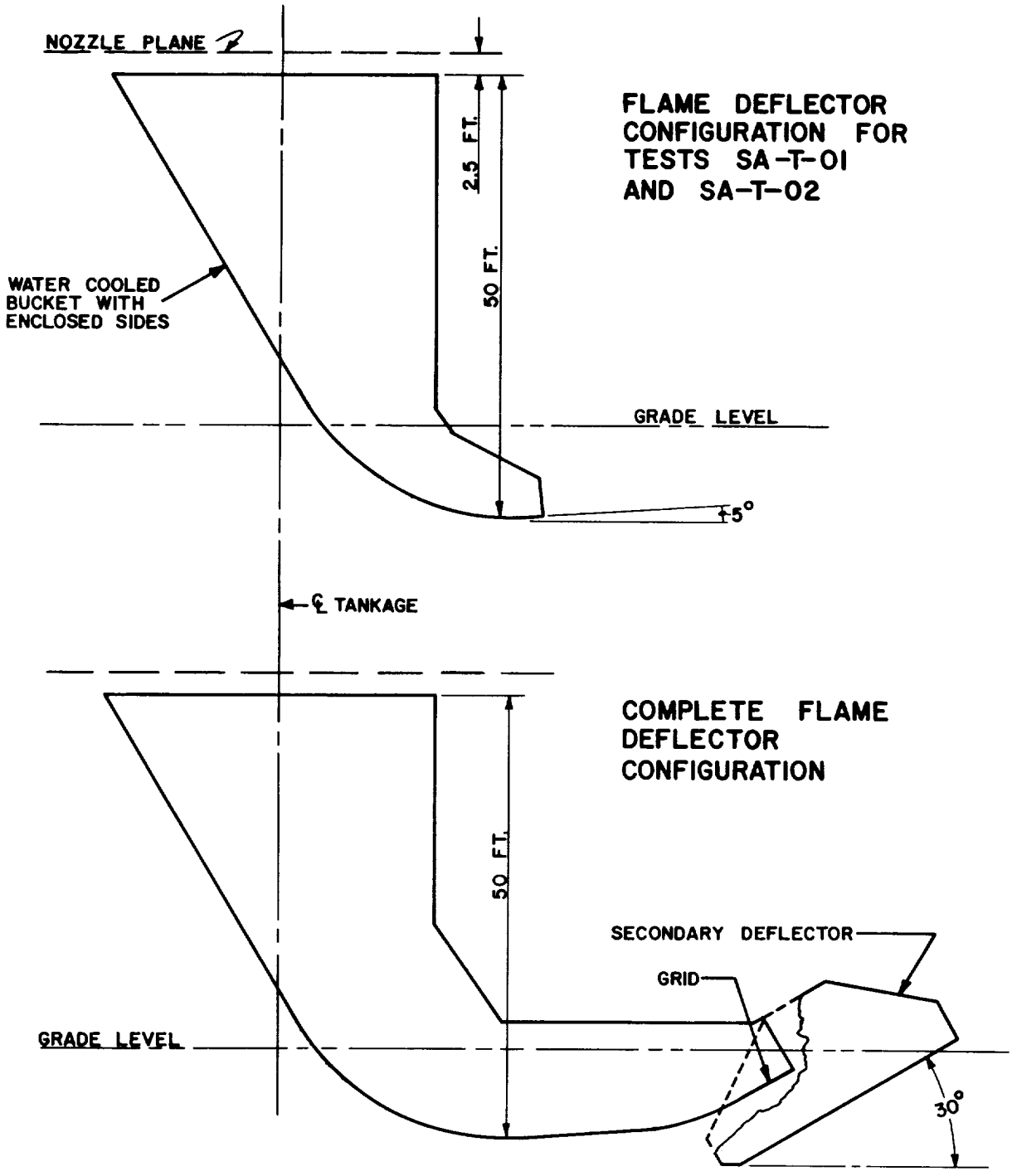

FIGURE 4 — SKETCH OF THE TWO DEFLECTOR CONFIGURATIONS

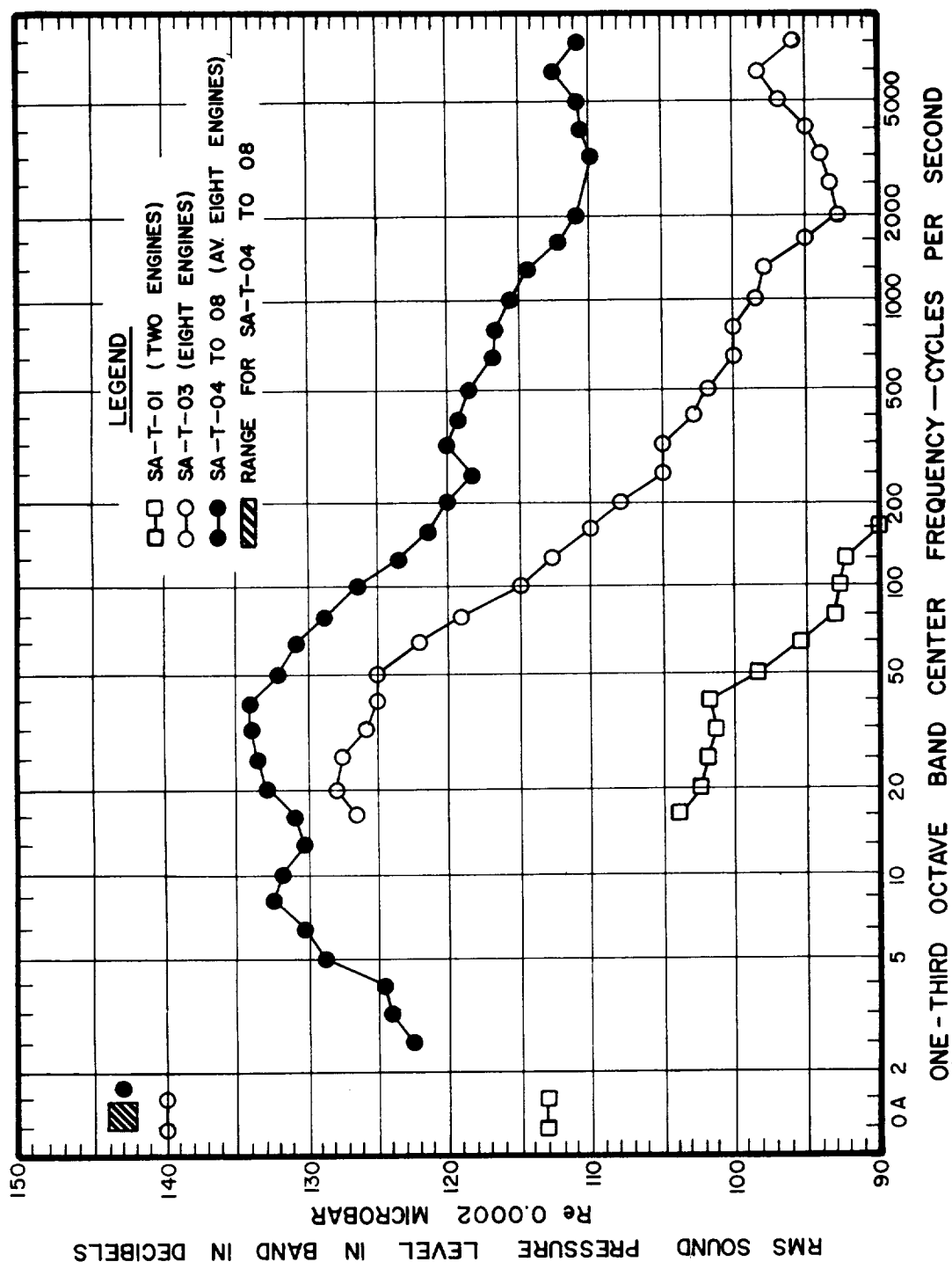

FIGURE 5 – SOUND SPECTRA AT 600 FOOT DISTANCE AND 0° ANGULAR COORDINATE

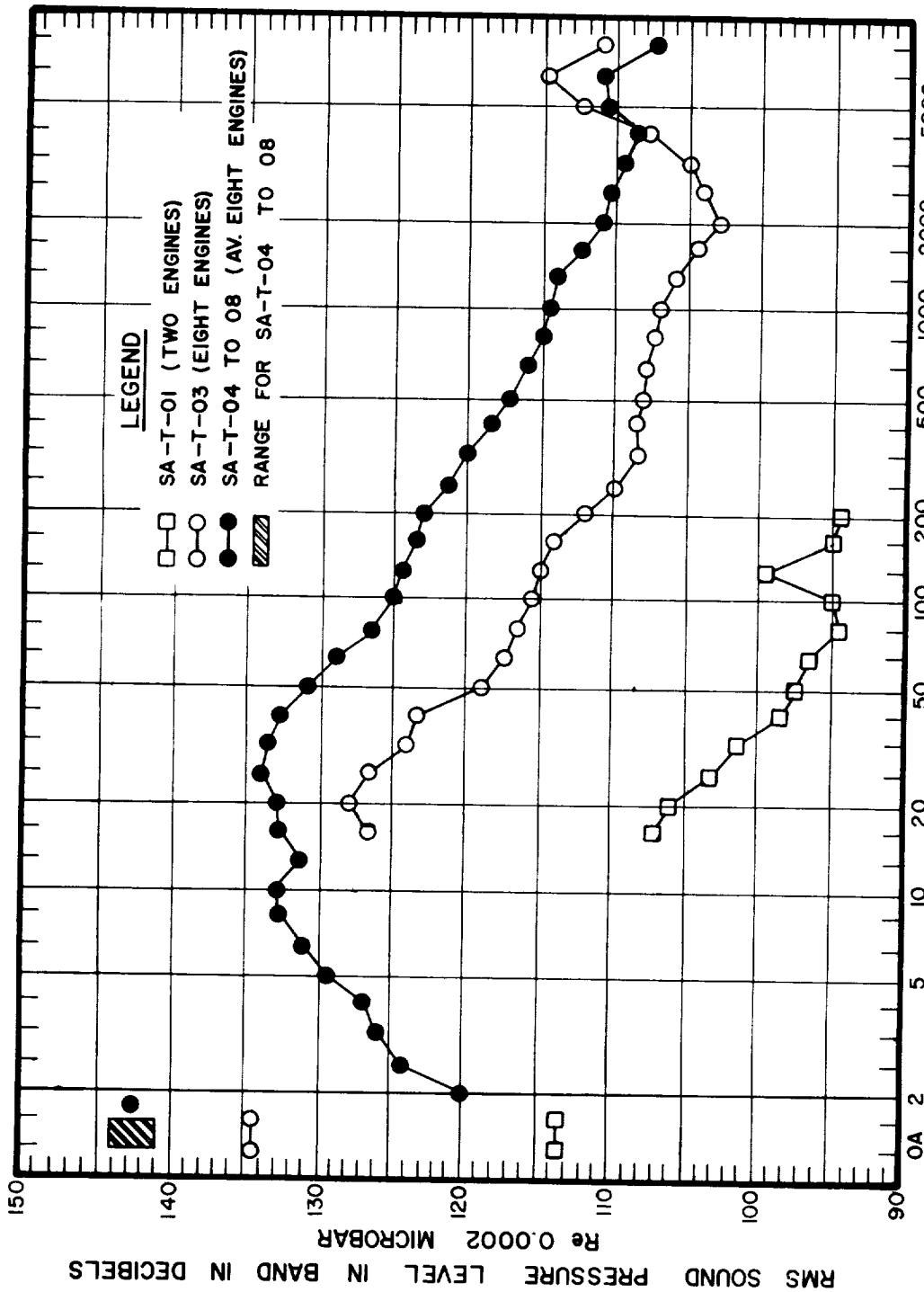

FIGURE 6 — SOUND SPECTRA AT 600 FOOT DISTANCE AND 10° ANGULAR COORDINATE

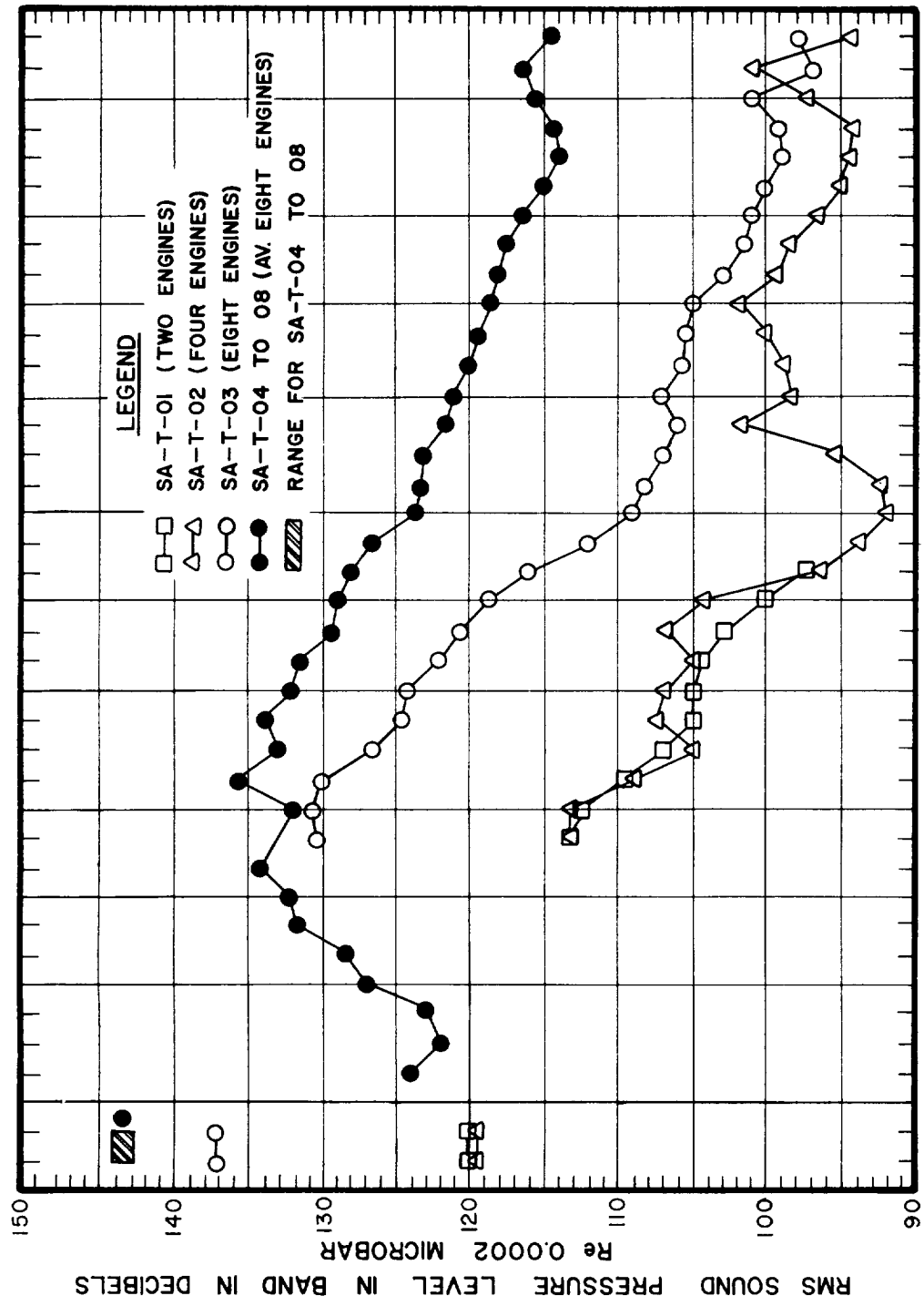

FIGURE 7 – SOUND SPECTRA AT 600 FOOT DISTANCE AND 20° ANGULAR COORDINATE

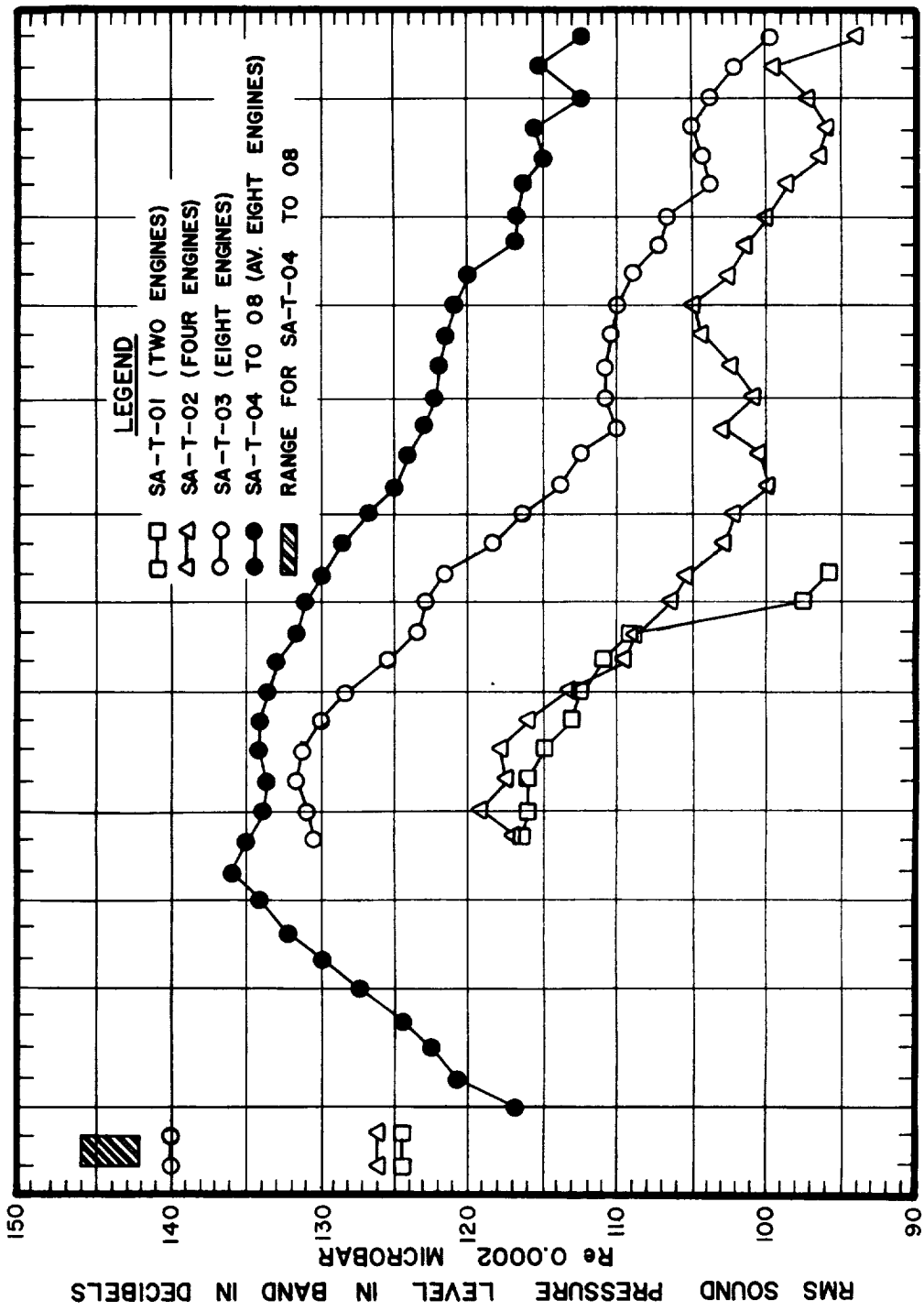

FIGURE 8 - SOUND SPECTRA AT 600 FOOT DISTANCE AND 30° ANGULAR COORDINATE

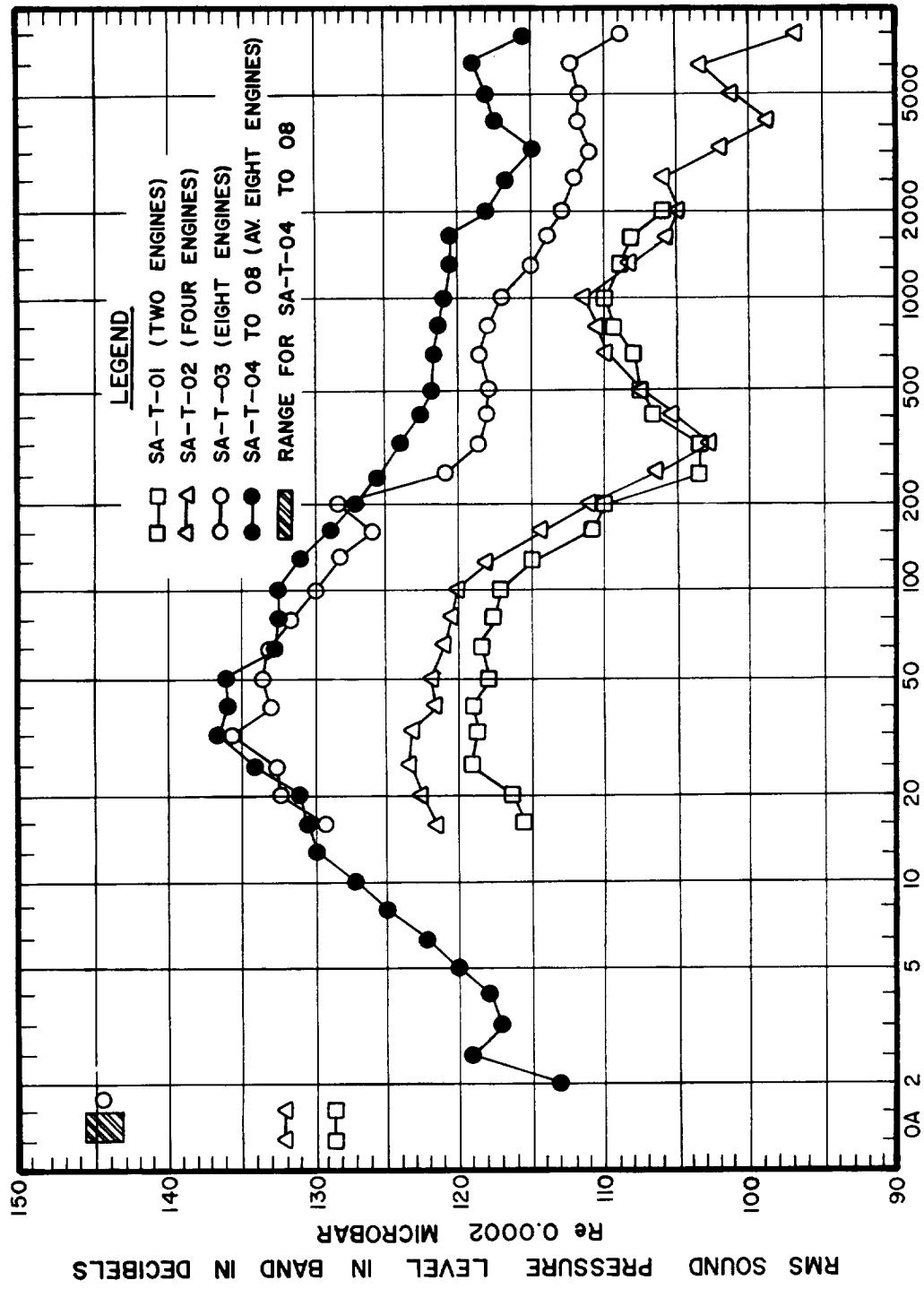

FIGURE 9 — SOUND SPECTRA AT 600 FOOT DISTANCE AND 50° ANGULAR COORDINATE

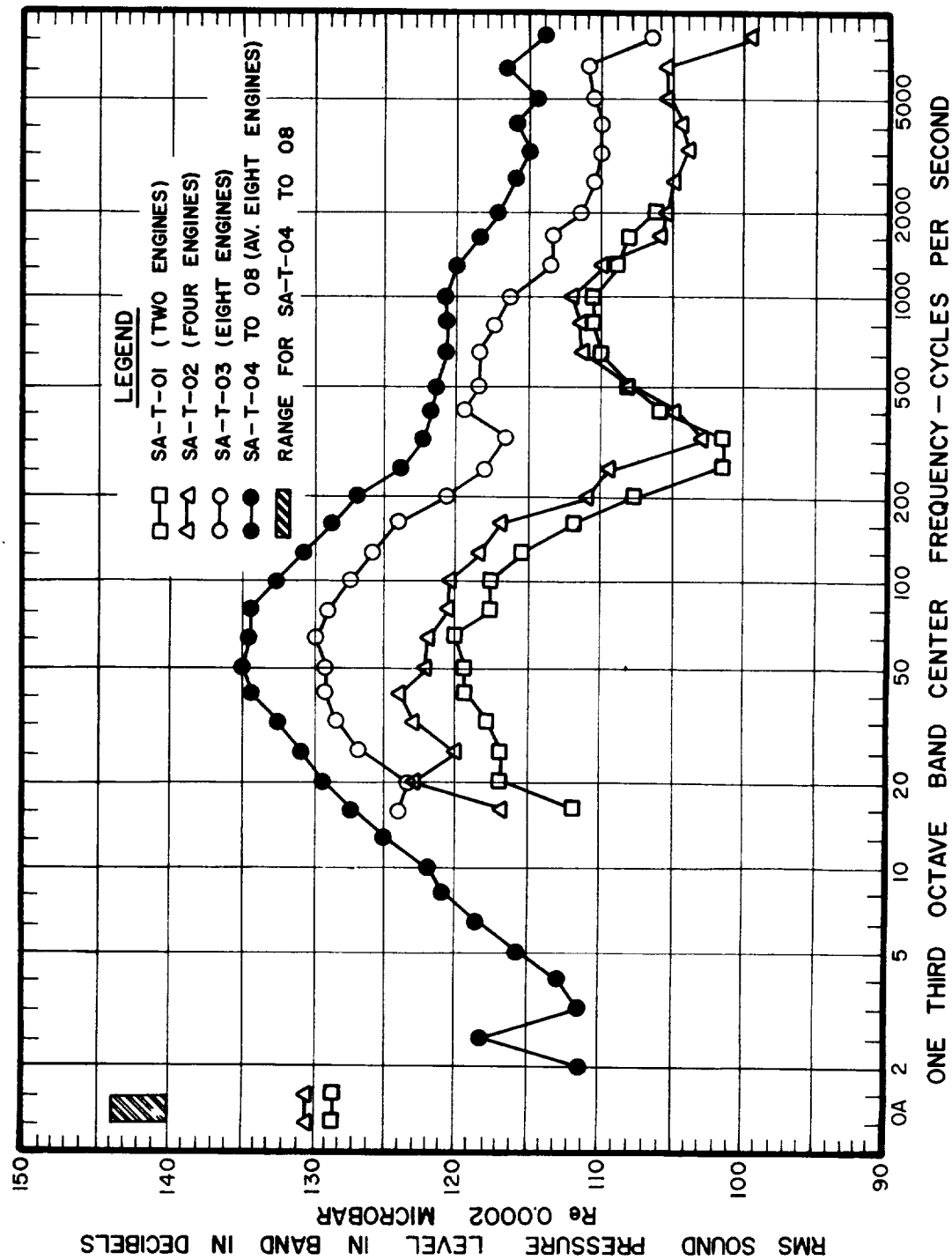

FIGURE 10 – SOUND SPECTRA AT 600 FOOT DISTANCE AND 60° ANGULAR COORDINATE

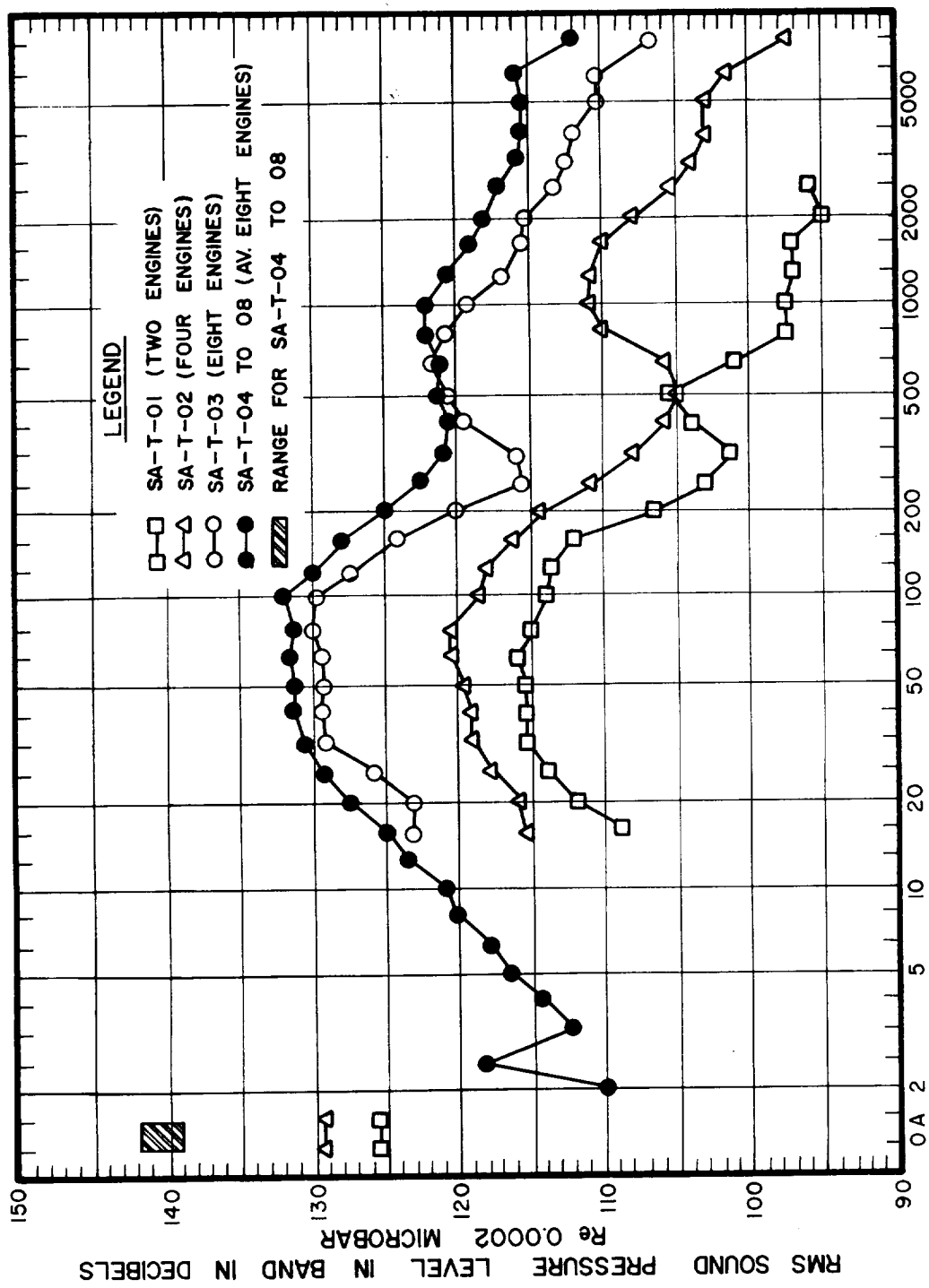

FIGURE 11 - SOUND SPECTRA AT 600 FOOT DISTANCE AND 70° ANGULAR COORDINATE

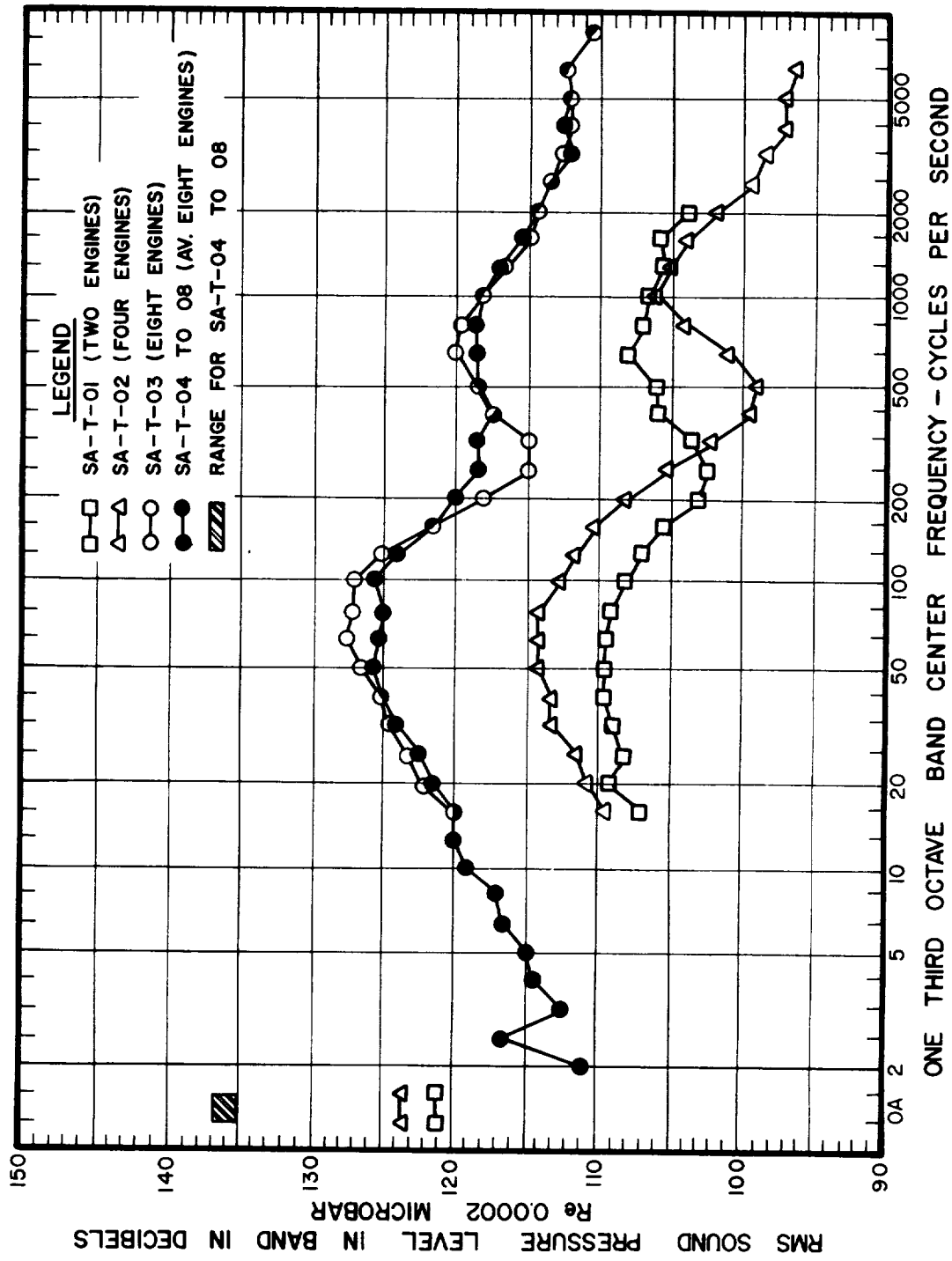

FIGURE 12 – SOUND SPECTRA AT 600 FOOT DISTANCE AND 90° ANGULAR COORDINATE

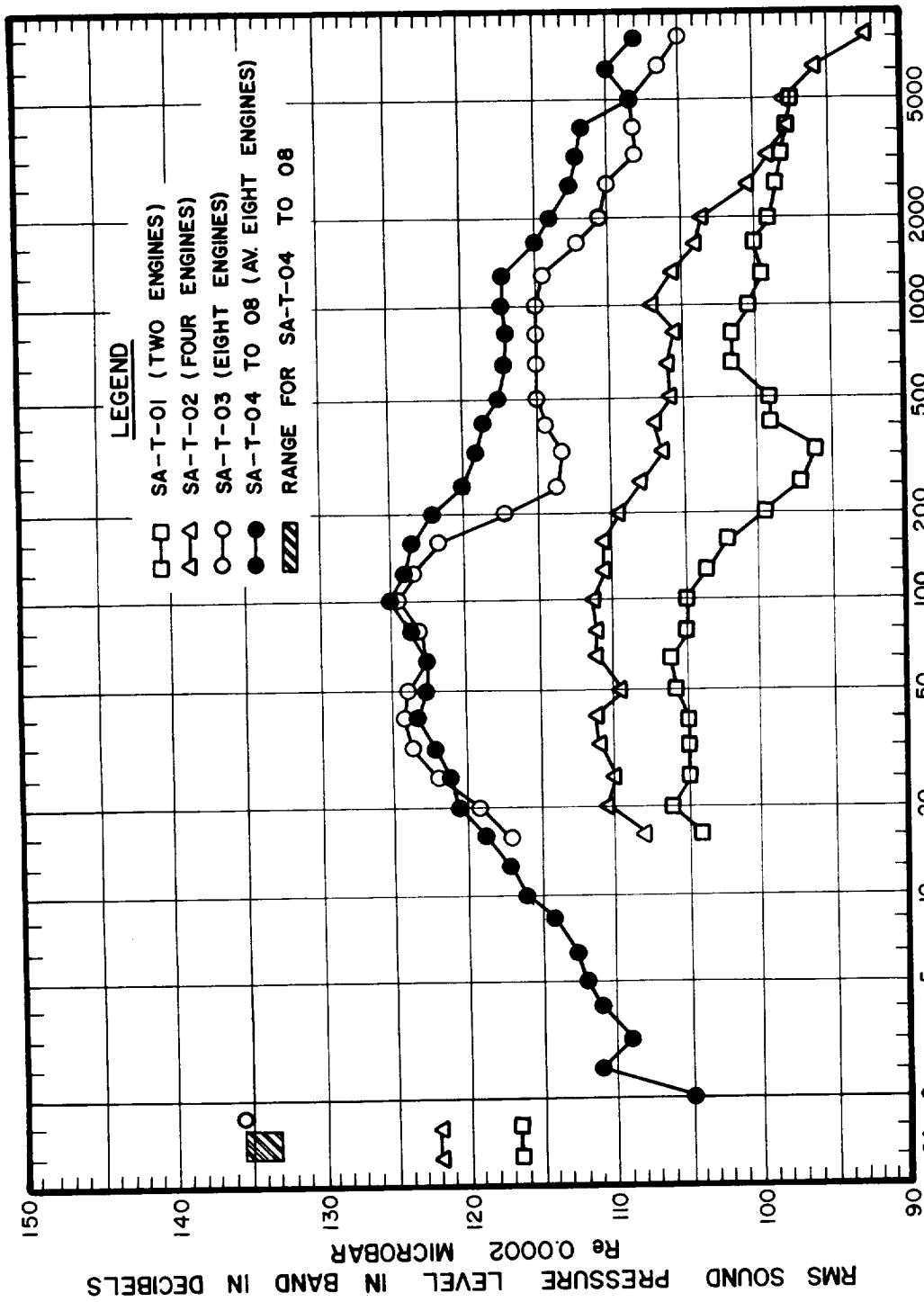

FIGURE 13 – SOUND SPECTRA AT 600 FOOT DISTANCE AND 110° ANGULAR COORDINATE

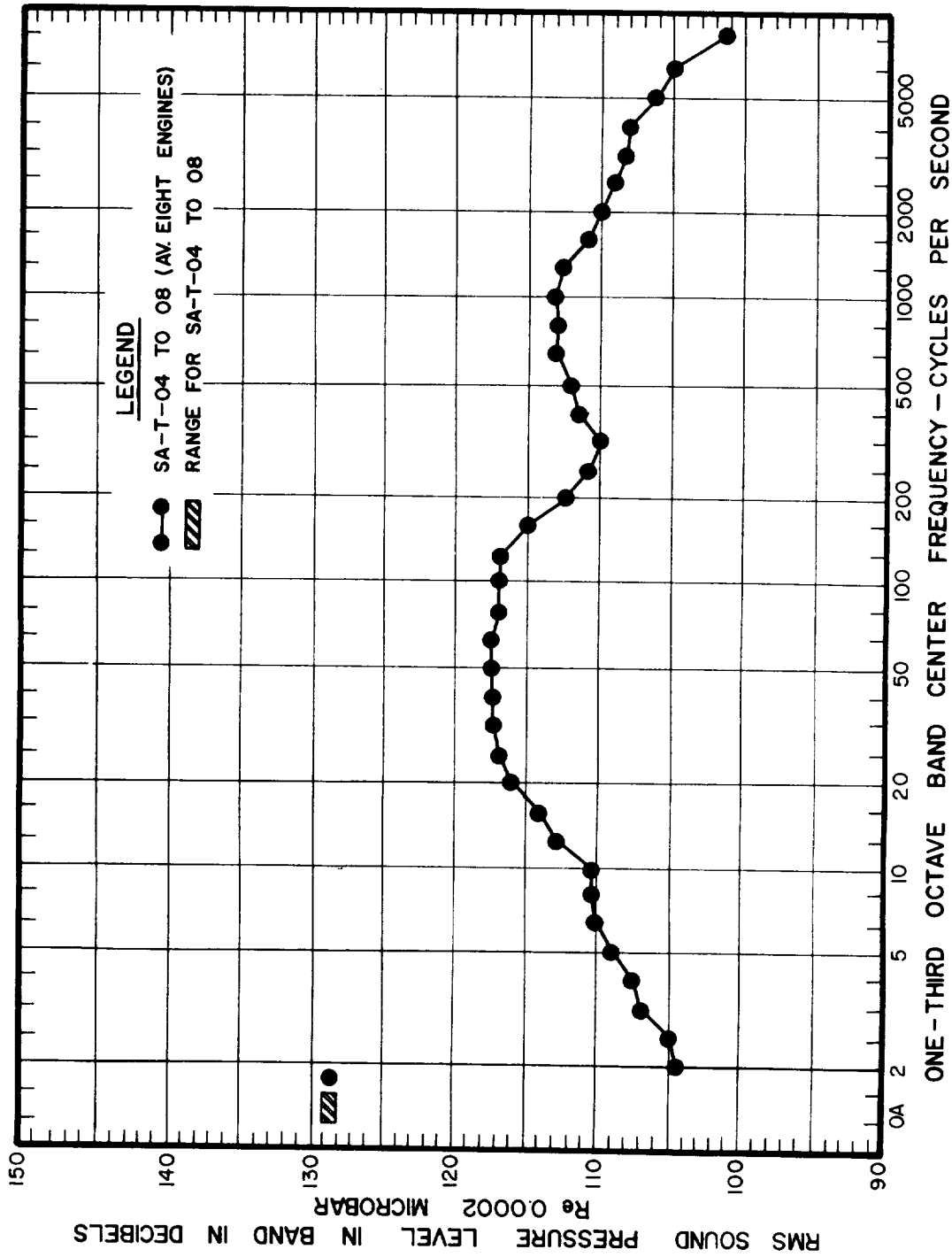

FIGURE 14 - SOUND SPECTRA AT 600 FOOT DISTANCE AND 150° ANGULAR COORDINATE

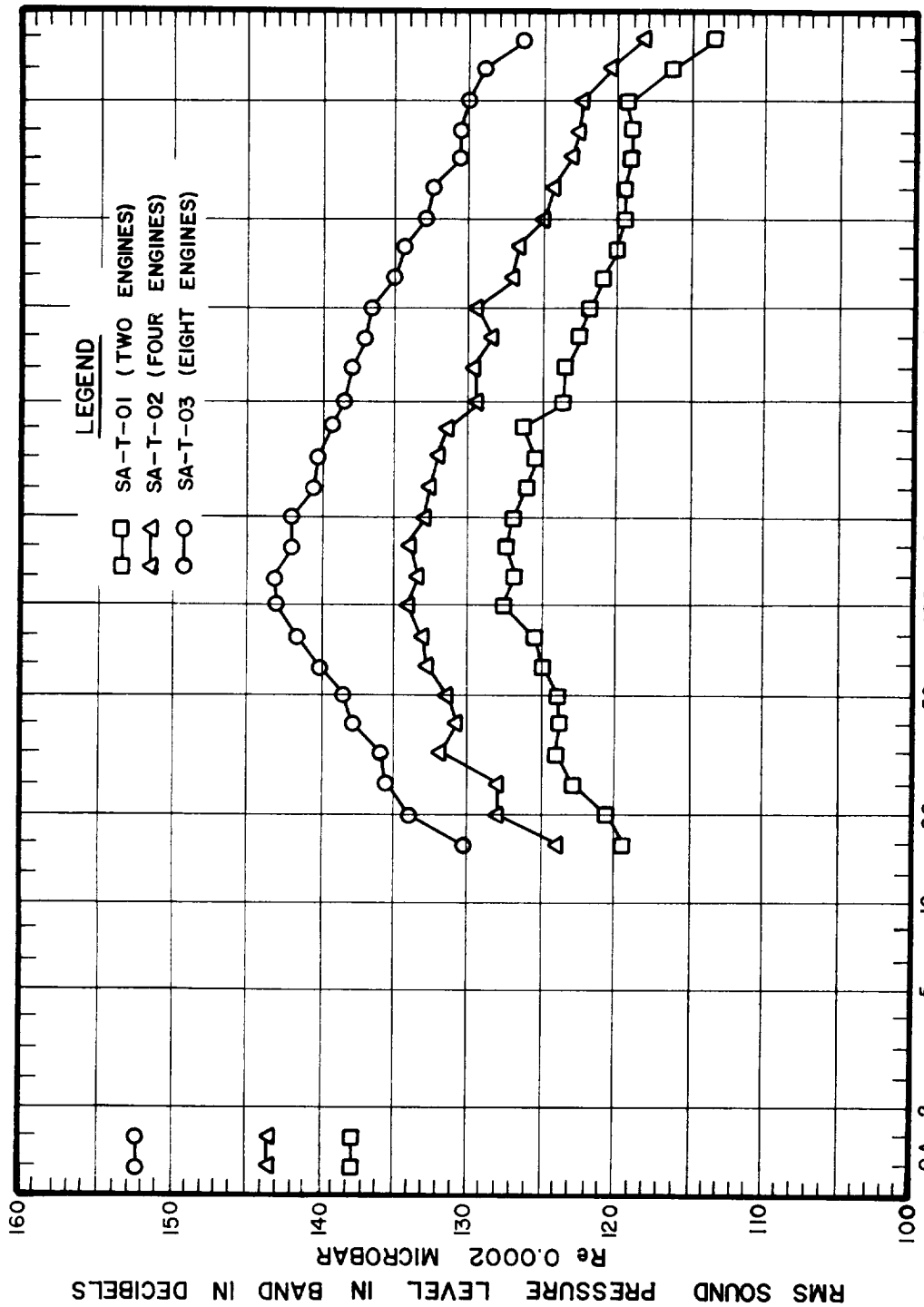

FIGURE 15 – SOUND SPECTRA AT 150 FOOT DISTANCE AND 60° ANGULAR COORDINATE

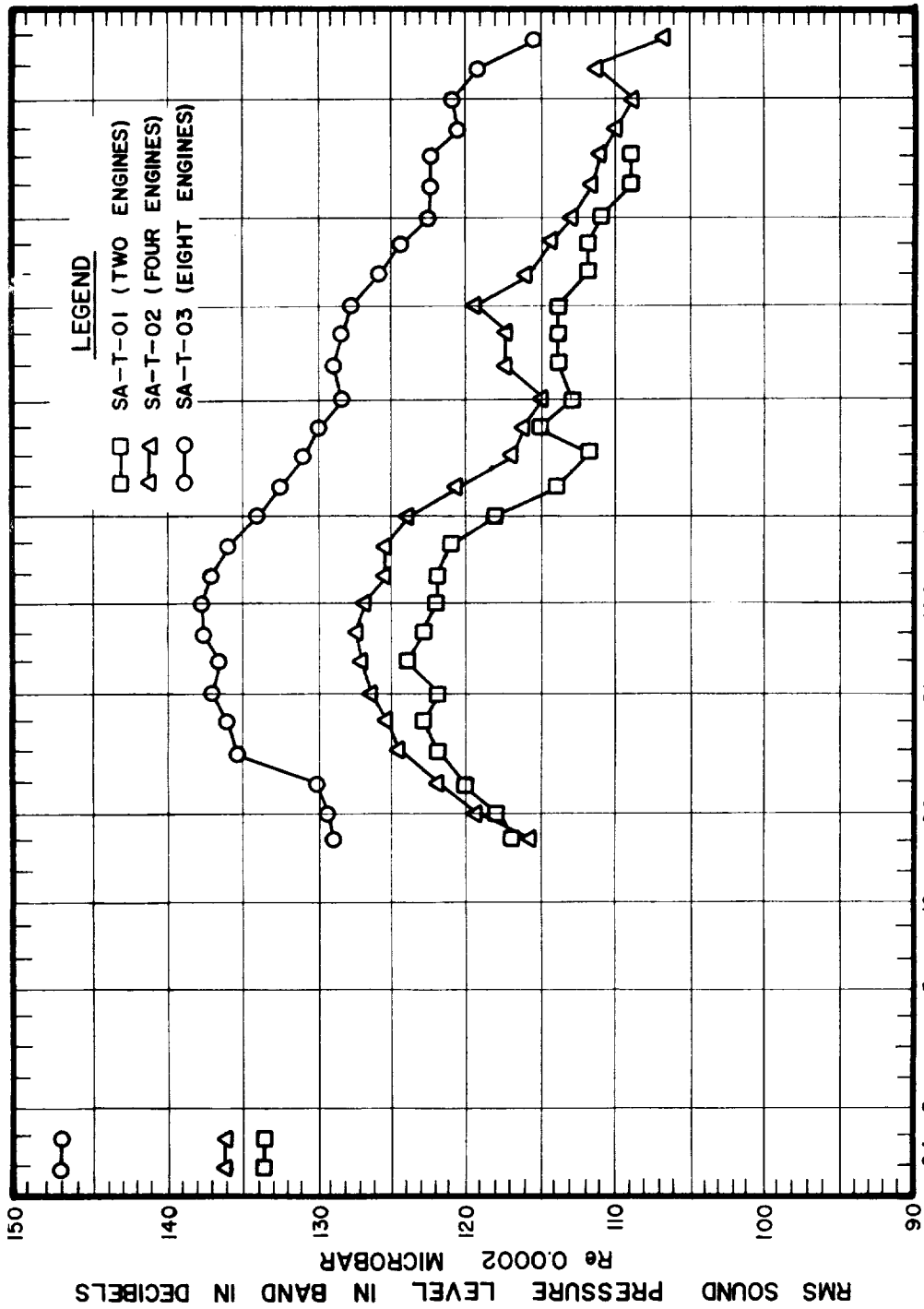

FIGURE 16 - SOUND SPECTRA AT 300 FOOT DISTANCE AND 60° ANGULAR COORDINATE

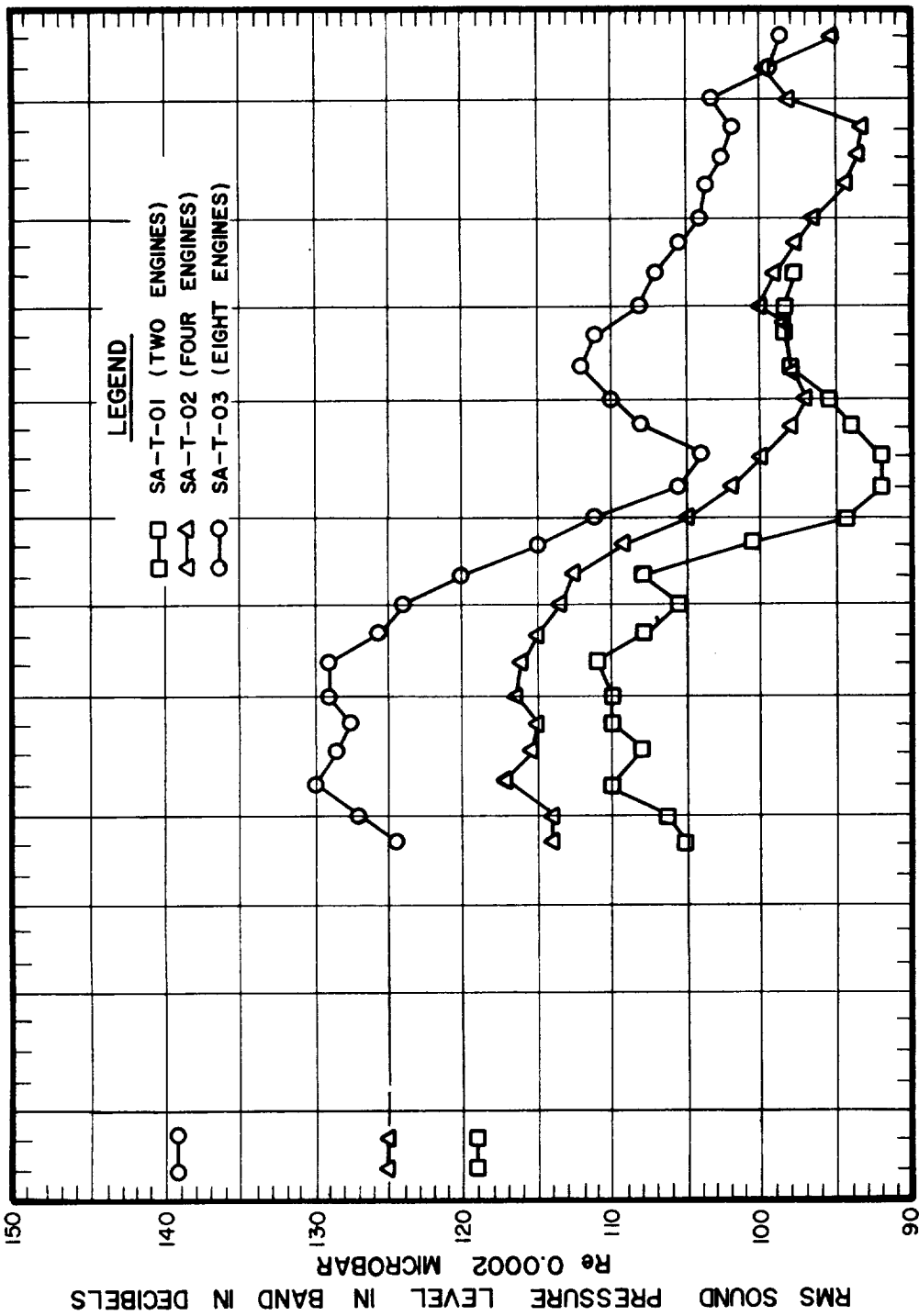

FIGURE 17 — SOUND SPECTRA AT 1200 FOOT DISTANCE AND 60° ANGULAR COORDINATE

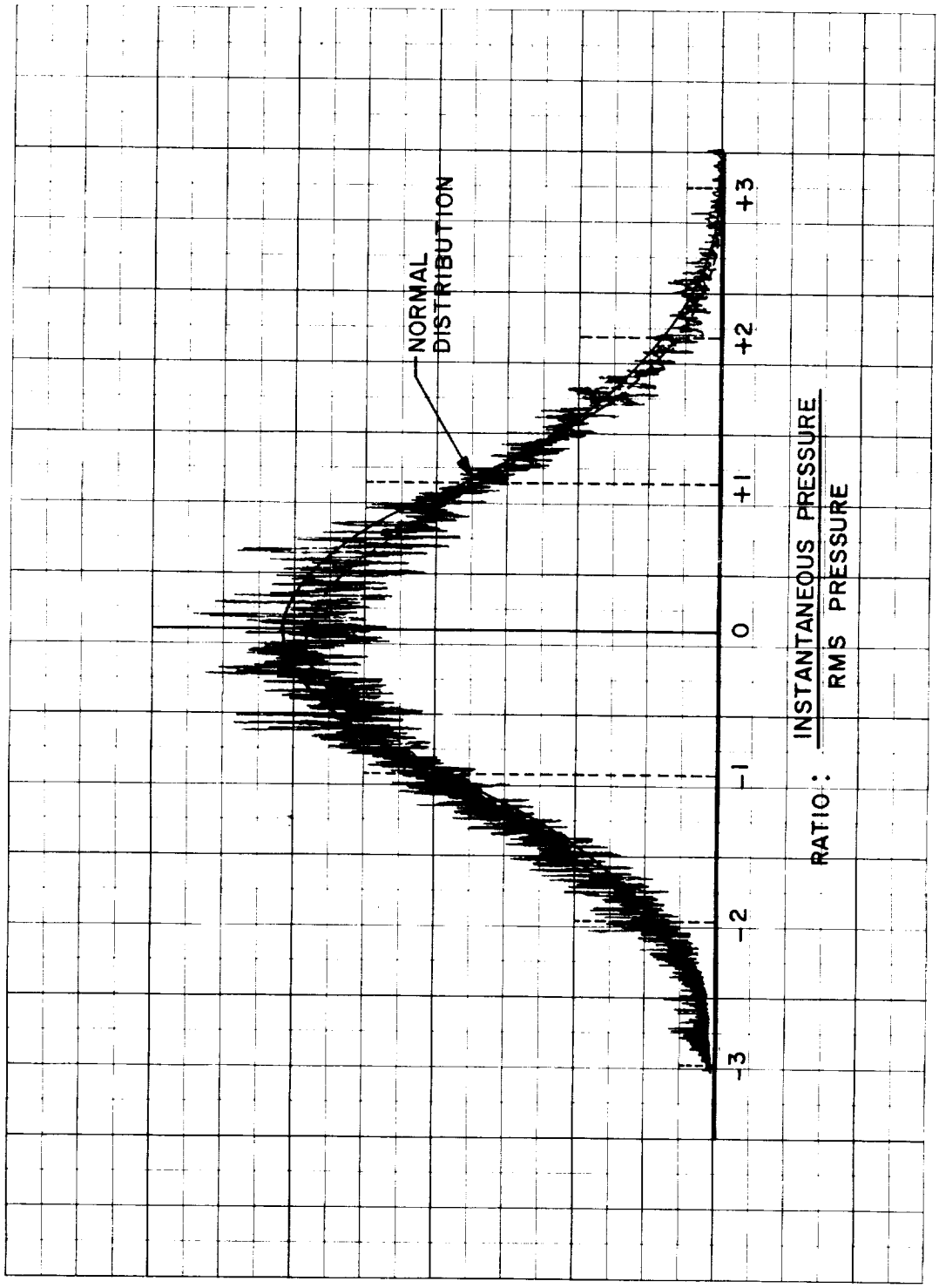

FIGURE 18: RELATIVE AMPLITUDE DISTRIBUTION OF ACOUSTIC NOISE MEASUREMENT RECORDED AT 600 FT, 0° DURING 8-ENGINE TEST OF SATURN BOOSTER

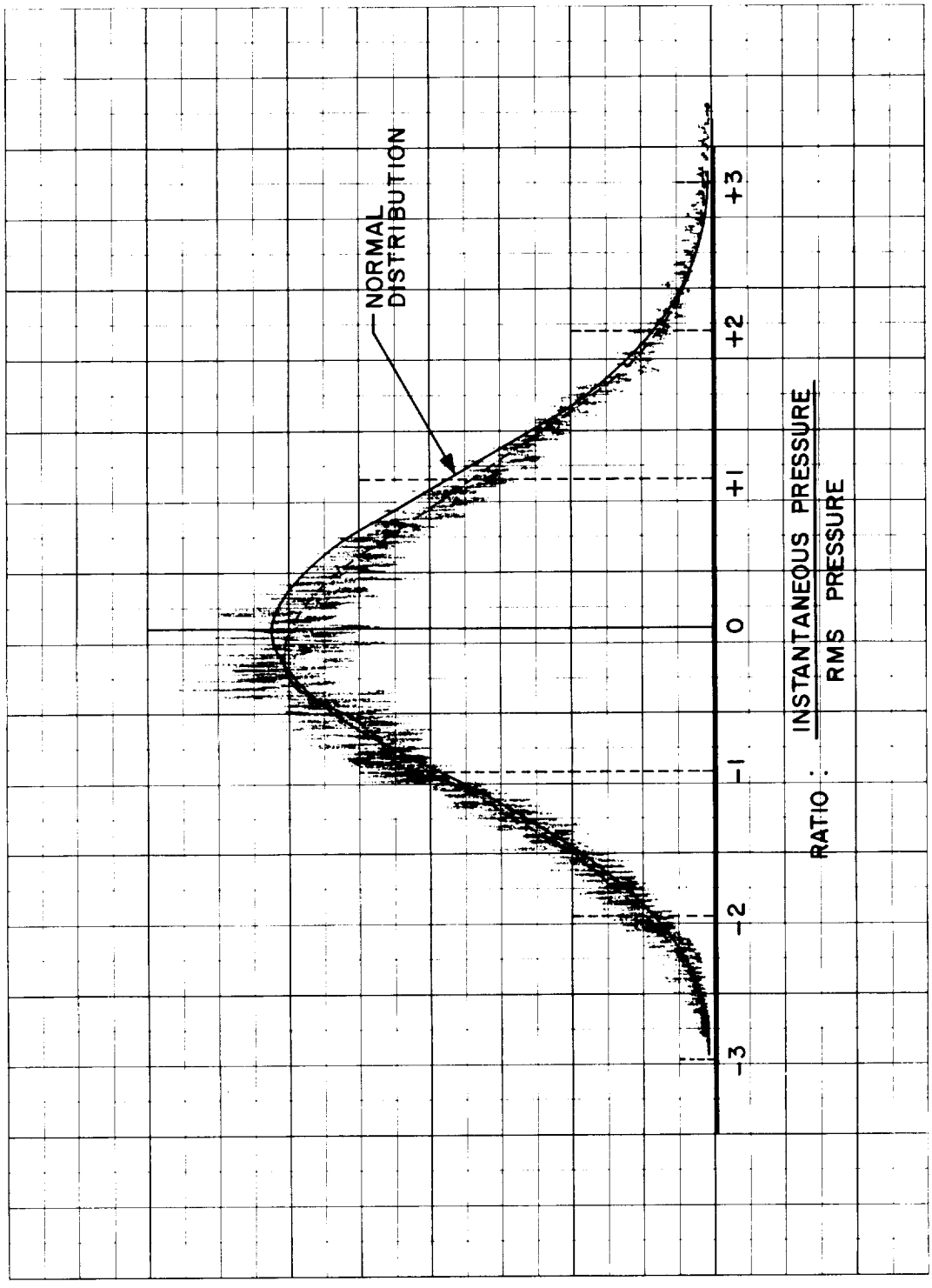

FIGURE 19: RELATIVE AMPLITUDE DISTRIBUTION OF ACOUSTIC NOISE MEASUREMENT RECORDED AT 600 FT, 20° DURING 8-ENGINE TEST OF SATURN BOOSTER

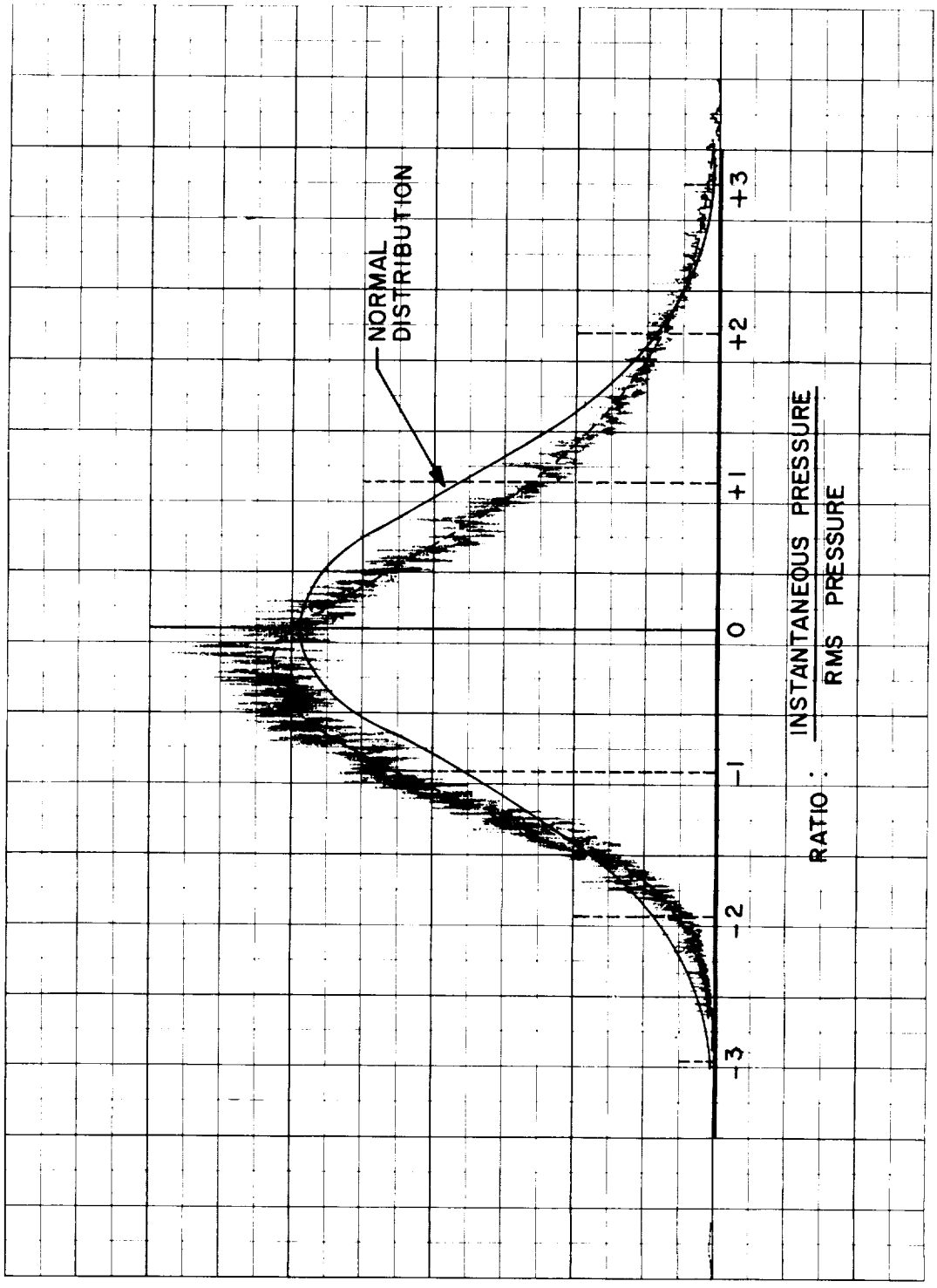

FIGURE 20: RELATIVE AMPLITUDE DISTRIBUTION OF ACOUSTIC NOISE MEASUREMENT RECORDED AT 600 FT, 60° DURING 8-ENGINE TEST OF SATURN BOOSTER

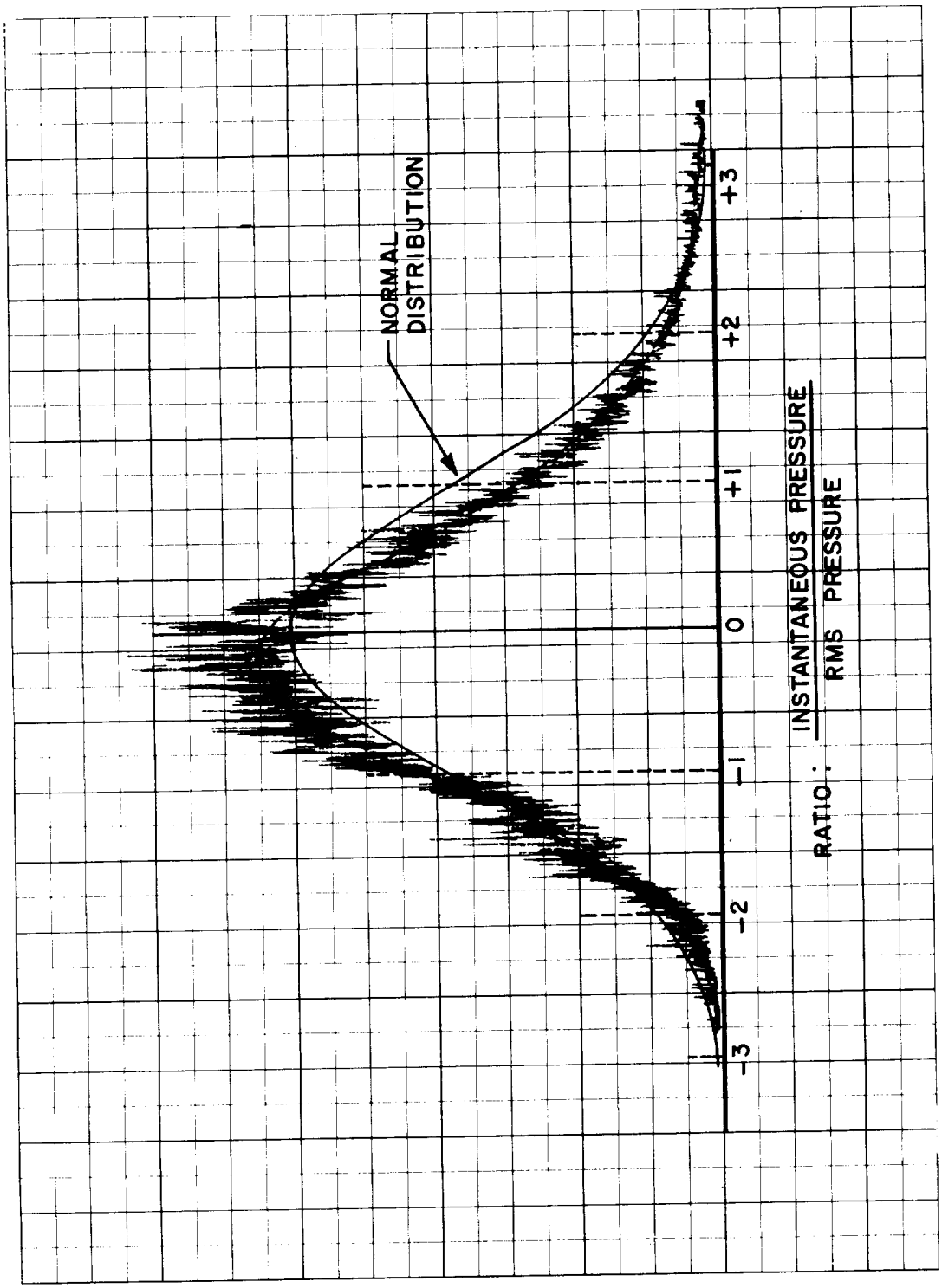

FIGURE 21: RELATIVE AMPLITUDE DISTRIBUTION OF ACOUSTIC NOISE MEASUREMENT RECORDED AT 1200 FT, 60° DURING 8-ENGINE TEST OF SATURN BOOSTER

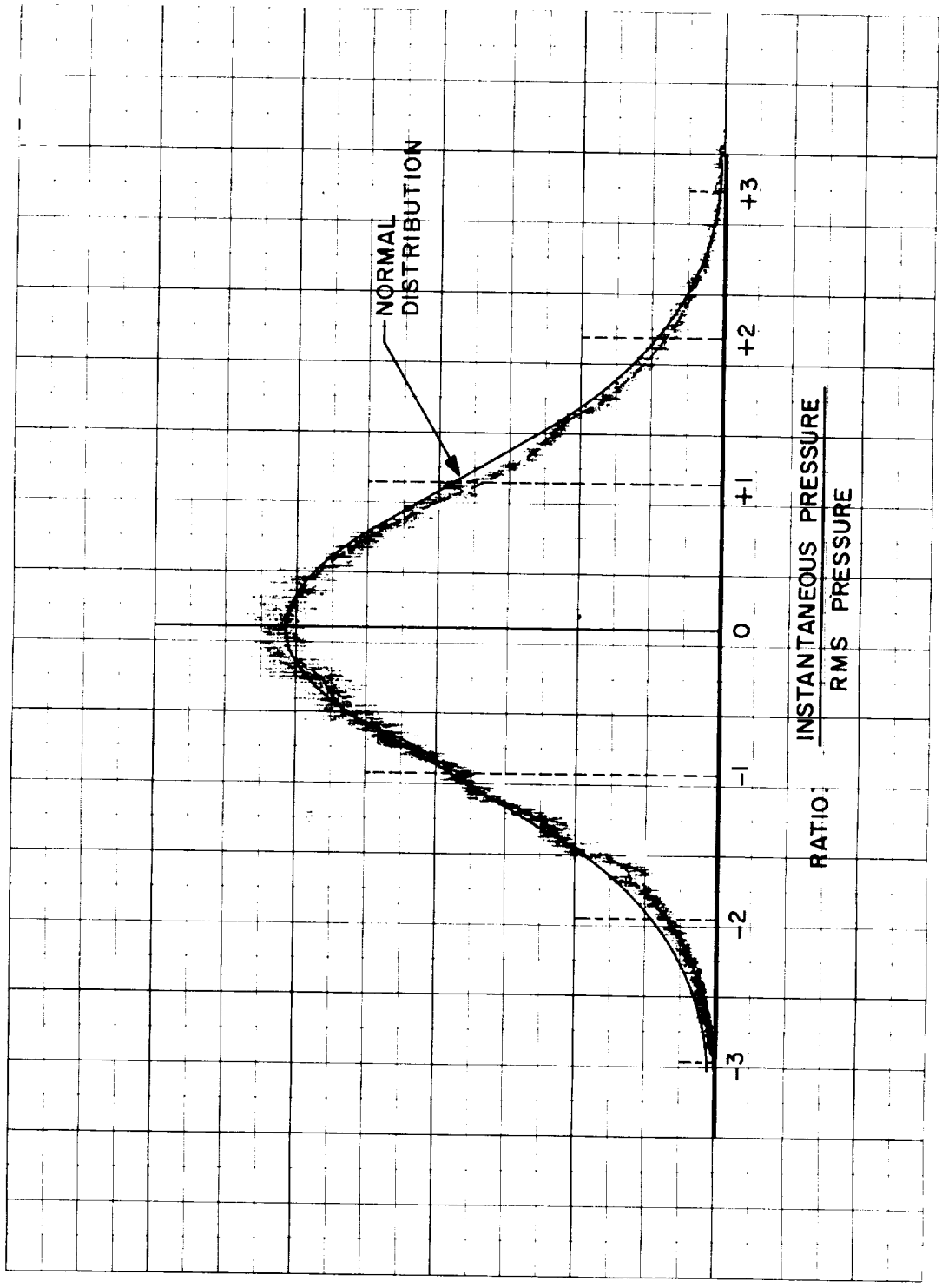

FIGURE 22: RELATIVE AMPLITUDE DISTRIBUTION OF ACOUSTIC NOISE MEASUREMENT RECORDED AT 600 FT, 110° DURING 2-ENGINE TEST OF SATURN BOOSTER

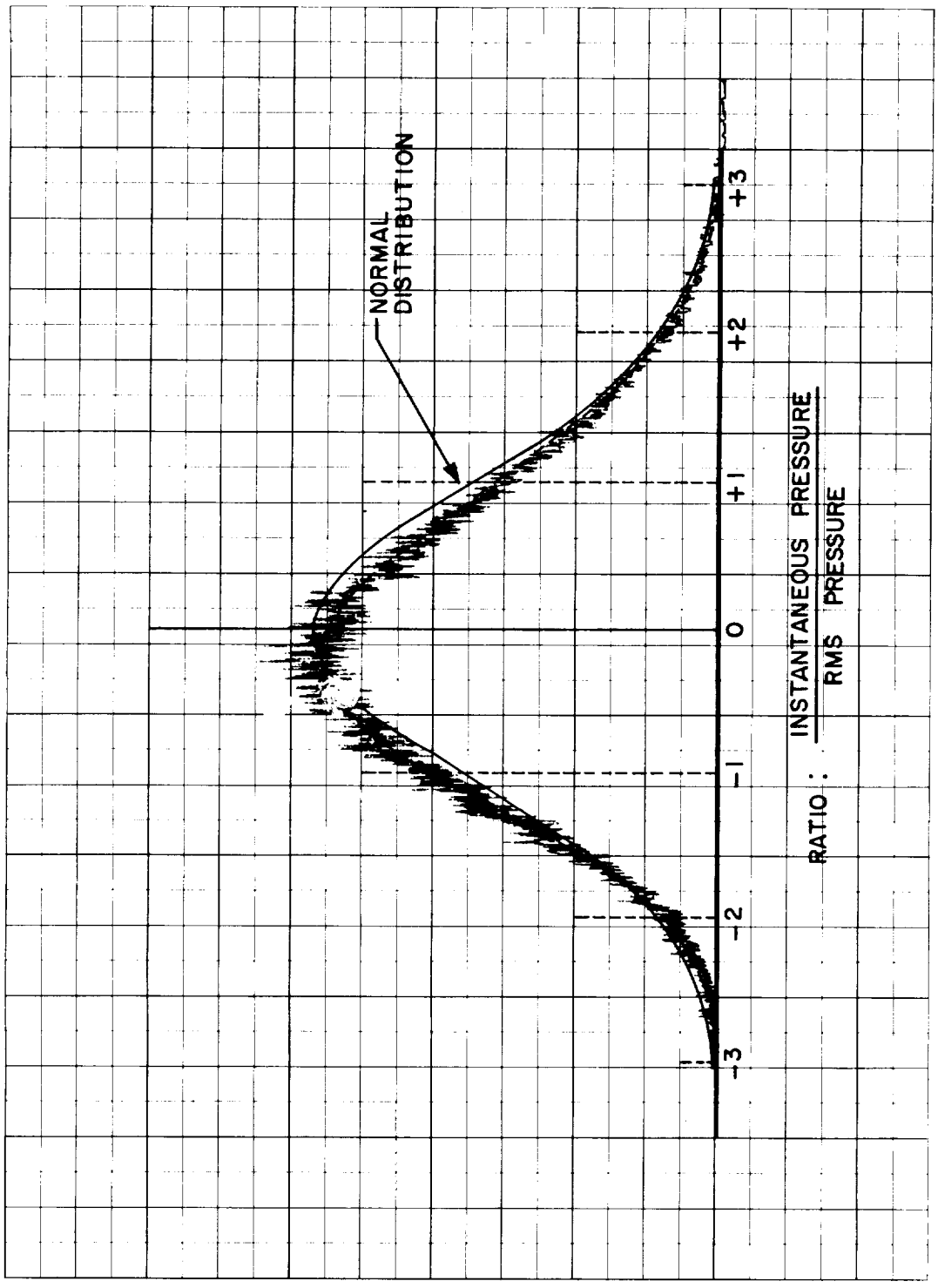

FIGURE 23 : RELATIVE AMPLITUDE DISTRIBUTION OF ACOUSTIC NOISE MEASUREMENT RECORDED AT 600 FT, 110° DURING 8-ENGINE TEST OF SATURN BOOSTER

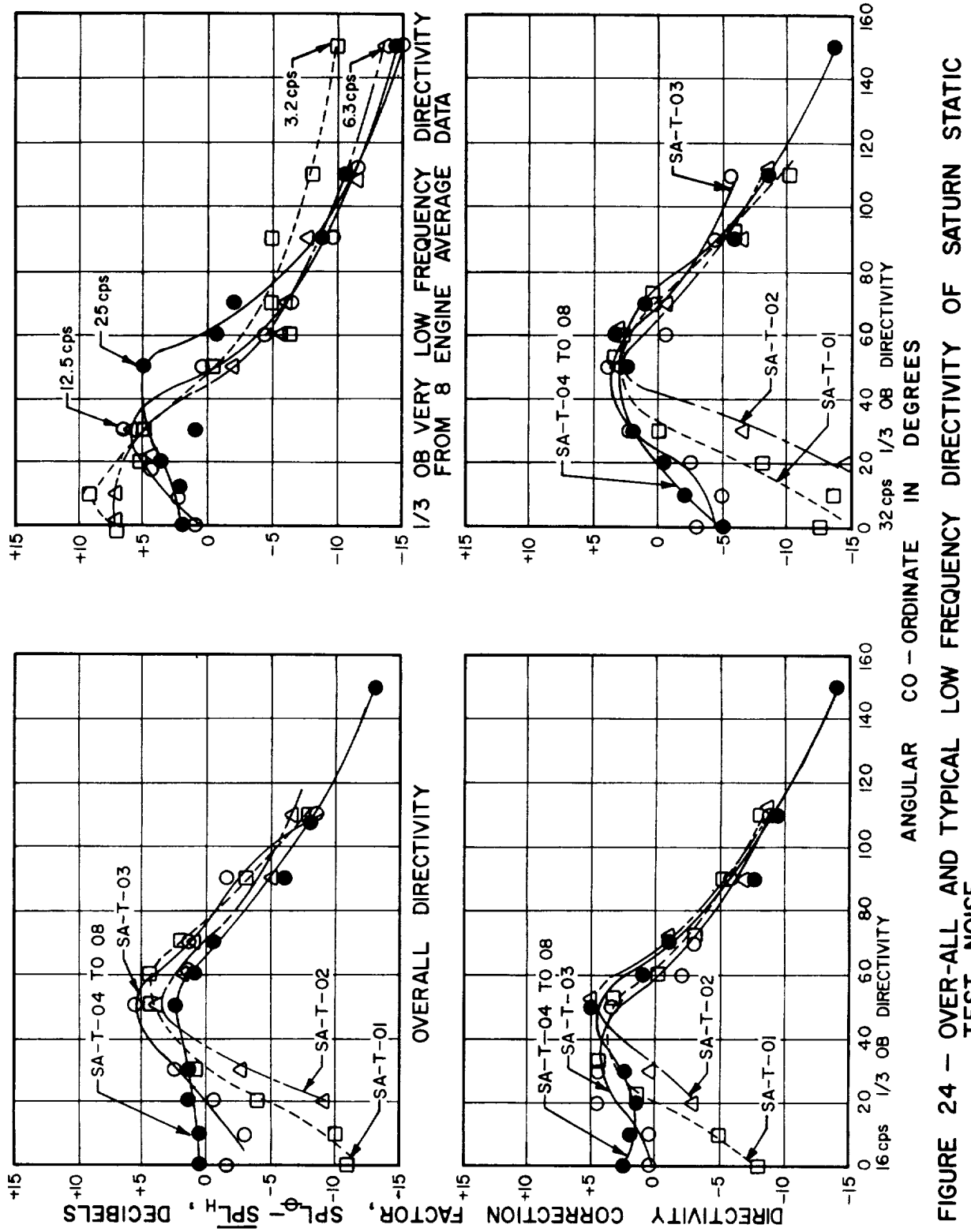

FIGURE 24 – OVER-ALL AND TYPICAL LOW FREQUENCY DIRECTIVITY OF SATURN STATIC TEST NOISE

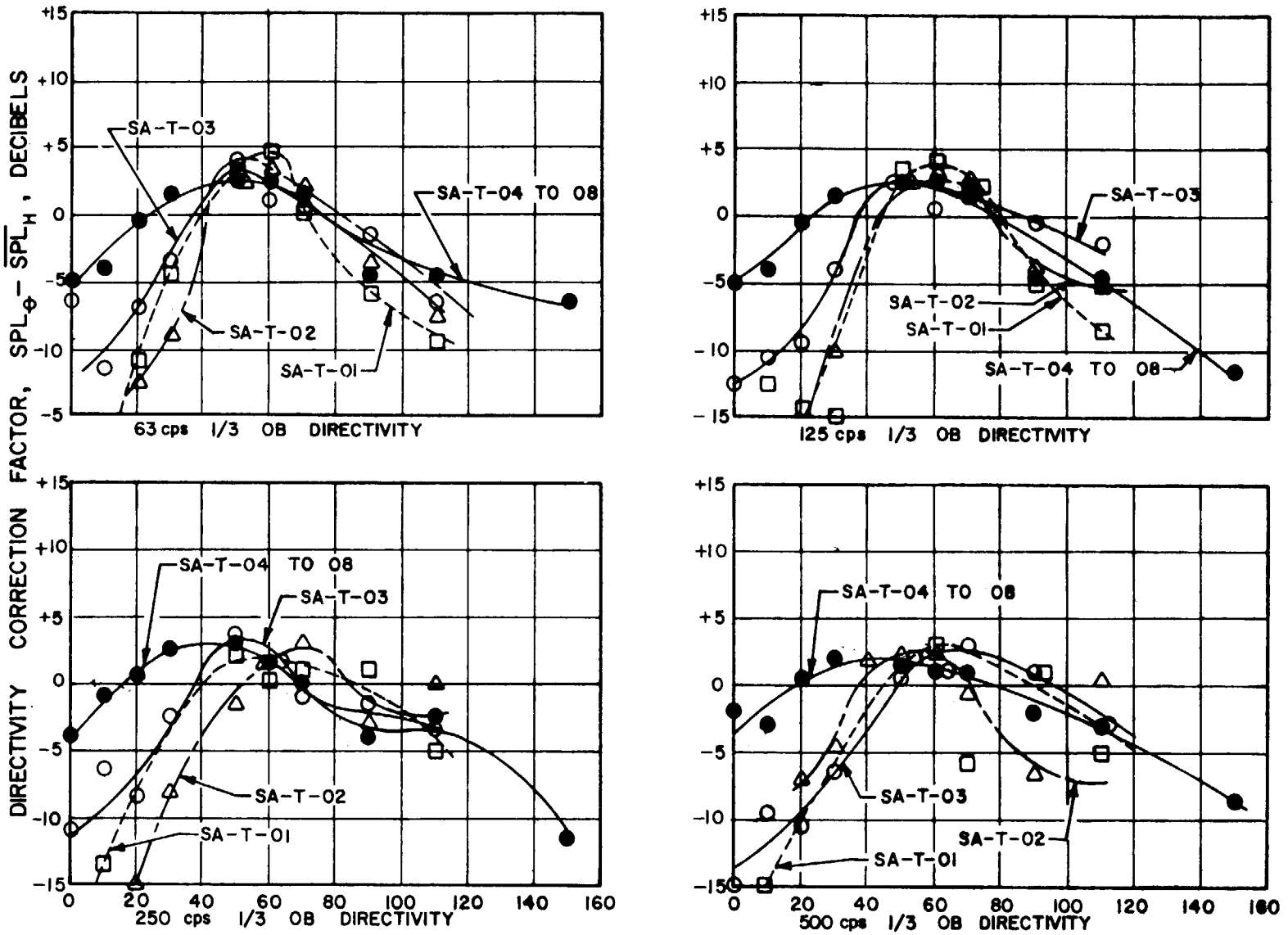

FIGURE 25- TYPICAL MIDDLE FREQUENCY DIRECTIVITY OF SATURN STATIC TEST NOISE

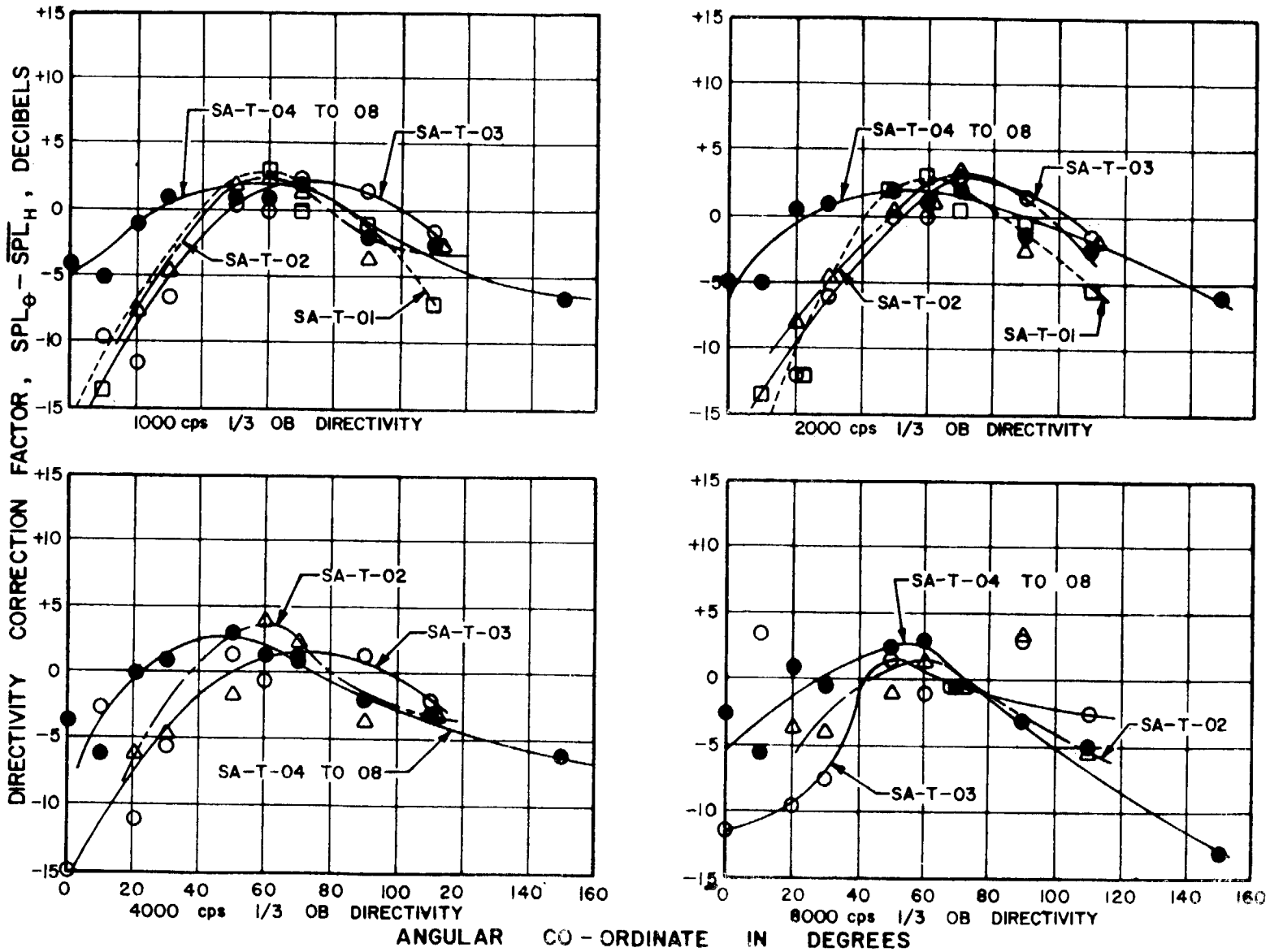

FIGURE 26 – TYPICAL HIGH FREQUENCY DIRECTIVITY OF SATURN STATIC TEST NOISE

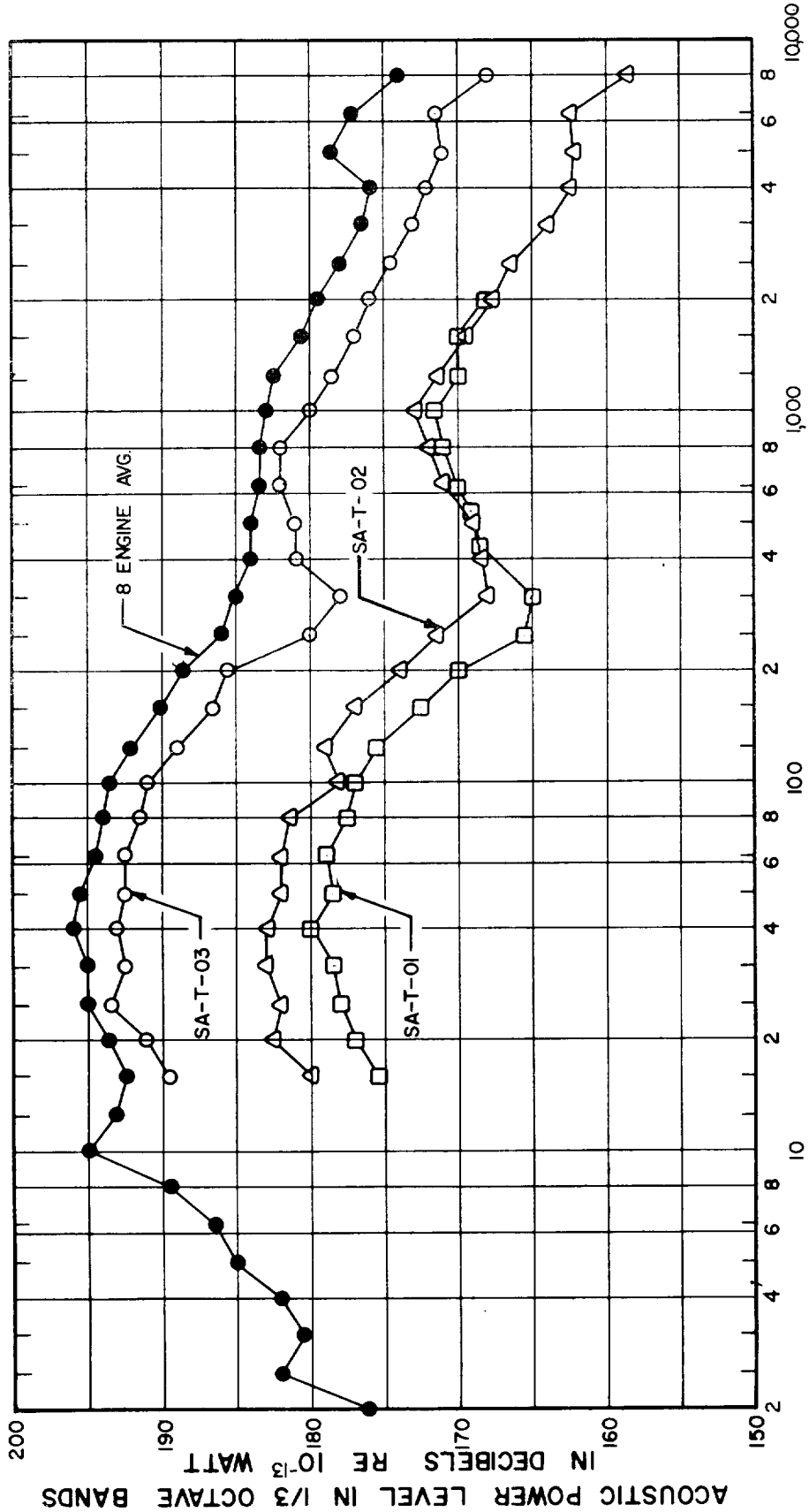

FIGURE 27 — POWER SPECTRA OF SATURN NOISE GENERATION IN VERY NARROW BANDS

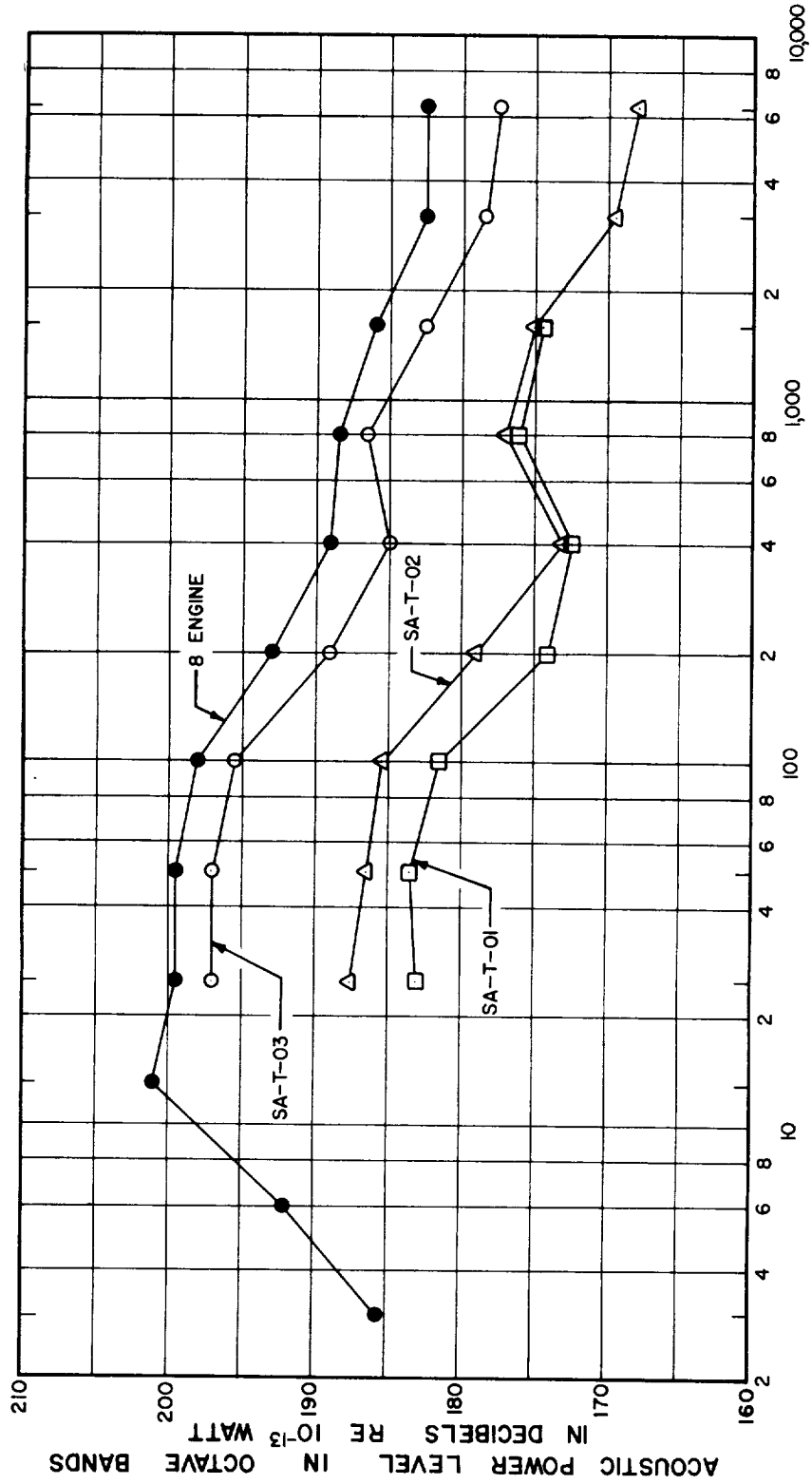

FIGURE 28 – POWER SPECTRA OF SATURN NOISE GENERATION IN NARROW BANDS

APPENDIX A

INSTRUMENTATION FOR DETERMINATION OF FAR-FIELD NOISE CHARACTERISTICS IN SATURN STATIC TESTS

DATA ACQUISITION SYSTEM

To obtain the data for this program, a system was required which could cope with very stringent operating conditions. Included among those conditions are:

(1) Wide spread of transducers.

(2) Long transmission cables.

(3) Frequency response from 2 cps to 10,000 cps.

(4) A dynamic range of 70 decibels.

(5) Minimum distortion desired.

(6) Exposure to weather.

(7) Necessity for good environmental stability.

A schematic of the system used, identifying various components, is presented as Figure 29 of this technical note. Operational characteristics of the system and adequacy of the data acquired have proven quite acceptable. The piezoelectric crystal microphone is weatherproof and relatively stable in operation. However, because of its low sensitivity and high internal impedance, a battery-driven preamplifier was placed at each measuring point. This allowed use of a short microphone cable, providing low noise signal boost and adequate power to drive the long transmission lines. A monitor and control amplifier matched incoming signals to the limited dynamic range of the tape recorder to produce excellent recording fidelity.

Before and after each test, a chamber was placed over each microphone and a calibration test made to produce a rms SPL of 130 db at 400 cps. The pre-run calibration was recorded on tape and used as a reference tone for data reduction. These stability checks revealed very little change in sensitivity over the entire period of survey and served to increase confidence in the system. Frequent checks were also made on dynamic range, linearity, frequency response, and distortion in the various components.

DATA REDUCTION SYSTEM

A thorough evaluation of sound data requires a frequency analysis of the recorded random signals. The evaluation of data for this survey is based upon a spectral distribution of the root-mean-square amplitudes of the sound waveforms. To obtain such spectra, measurements were assumed to be constant over the test duration. A sample was then taken from each measurement and processed to produce the data required.

A schematic of the data reduction system is shown on Figure 29. A loop recorder is used to obtain a data sample four to six seconds in length and the rest of the system then analyzes the sample. All mathematical functions of squaring, integrating, and computing roots are performed by the system. This provides a "true rms" method of analyzing and produces the rms amplitude of a signal, regardless of its waveform. The spectrometer breaks the spectra into frequency bands one-third octave wide, giving data narrow enough for good spectral resolution, but wide enough for good statistical accuracy. Automatic switching systems, controlled by sample length, provide rapidity in analyzing data and accurate control of integration time.

Because of limitation in the spectrometer filter system, the speed multiplication feature of the loop recorder is utilized to reduce signals below 16 cps. A signal recorded at 7½ ips is played back at 60 ips. This gives a frequency multiplication factor of 8 and allows a 2 cps signal to pass the 16 cps filter in the spectrometer. One disadvantage of this procedure is that a 5-second loop at 60 ips requires 40 seconds of recorded data at 7½ ips. Thus, data from tests of less than 40 seconds duration cannot be analyzed below 16 cps.

To evaluate randomness of noise waveforms recorded during this survey, selected data were analyzed using a probability density analyzer which produces a plot of the amplitude distribution. The instrument was available for a limited time only, so the selected data gives a tentative, but not necessarily conclusive, evaluation of randomness. The mean curve for a given signal was drawn by inspection and the area under it measured with a polar planimeter. For reference, a Gaussian curve with the same area between ±3 sigma was then superimposed on the plot. Results are shown on Figures 18 to 23.

As with other phases of the instrumentation, frequent checks were made on all components to maintain precision and to establish confidence in the system.

PROJECT ACCURACY

Confidence in the accuracy of the recorded data, and in the values computed from it, is based on two things: precision of measurements, and proper consideration of the range of dispersion of the measurements. Use of extreme care in all operations and maintenance of a continuing check of components has resulted in a high degree of precision. Data for the eight-engine tests were averaged and as a result, the range of dispersion is obtained. Ranges found during the survey are shown on Figures 30 to 32. Considering all characteristics of the program, the following evaluation of accuracy is given:

(1) Data points shown on the pressure spectra are within ± 3 decibels of the true mean for 95% of the data.

(2) Data points shown on the pressure spectra are within ± 2 decibels of the true mean for 70% of the data.

(3) General confidence level is 95%.

APPENDIX B

CALCULATION OF DERIVED PARAMETERS

Averaging the individual measurements to produce the space average sound pressure level ($\overline{SPL_H}$) is done over the hemisphere area used in the survey. The equation for this operation is:

$$\text{Antilog}\ \frac{(\overline{SPL_H})}{10} = \frac{\sum_j (S_j)\ \text{Antilog}\ \frac{(SPL_j)}{10}}{S_{Total}} \qquad \text{(B1)}$$

where S_{Total} = total area of measurement array,

S_j = area associated with individual measurements,

SPL_j = SPL measured at individual positions, and

$\overline{SPL_H}$ = space average sound pressure level.

Once the space average sound pressure level is known, the directivity of the source can be found by comparing the individually measured SPL's to the $\overline{SPL_H}$ according to the expression:

$$DCF = SPL_j - \overline{SPL_H} \qquad \text{(B2)}$$

where DCF = the directivity correction factor. SPL_j and $\overline{SPL_H}$ are the same as for equation (B1).

The space average sound pressure level is also the basis for the computation of the power. Assuming the radiation obeys the inverse square law, then the power level at the source is the known space average SPL, plus the attenuation from the spreading due to inverse square law propagation within the hemisphere. In symbols, this is:

$$PWL = \overline{SPL_H} + 10 \log 2\pi R^2. \qquad \text{(B3)}$$

However, for the microphone array on the 600-foot arc, the equation can be simplified to:

$$PWL = \overline{SPL_H} + 63.5 \text{ in decibels power relative to } 10^{-13} \text{ watts.} \qquad \text{(B4)}$$

While this equation is only approximate, it is well within the operating accuracy of the project if normal pressure, temperature, and a quiet medium are assumed. By use of this operation, the power levels for the overall, one-third octave, and octave band spectra are readily calculated. The space average spectra were not plotted because the power spectra are the same, except for the vertical scale factor.

To calculate the octave band results, a procedure was used where the one-third octave pressure levels were converted to spectrum levels by use of suitable correction factors. Then three spectrum levels for each octave band were averaged and the octave band levels were calculated by use of bandwidth corrections. From the space average SPL's in octave bands, the power level was readily calculated with equation (B4). Details on this procedure can be found in References 9 and 10.

Using the formula, the acoustic efficiency was computed as

$$\eta = \frac{P_a}{P_m} \qquad \text{(B5)}$$

where P_a = acoustic power generated, in watts, and

P_m = kinetic energy in the jet stream per second.

Kinetic energy was computed from:

$$P_m = \tfrac{1}{2} MV^2 = \tfrac{1}{2} \frac{T^2}{M} = \tfrac{1}{2} \frac{gT^2}{W} = 16.1 \frac{T^2}{W} \qquad \text{(B6)}$$

where $V = T/M$ and

V = expanded jet velocity in feet per second,

T = measured thrust in pounds, and

M = mass flowrate in slugs per second. (A slug is defined as weight in pounds divided by acceleration of gravity in feet per second per second.)

W = weight flowrate in pounds per second.

Actual jet stream velocity is only approximately equal to the expanded jet velocity (T/M), because the stream pressure in a fully-expanded flow does not equal the ambient pressure. However, until more data on the jet stream pressure are available, the approximation will be considered valid with an estimated error of less then 10 percent.

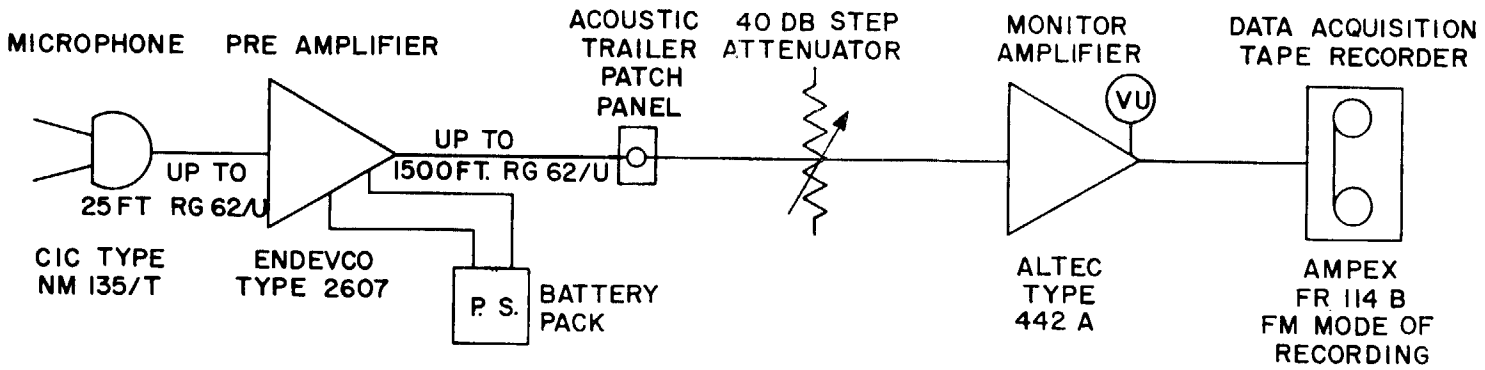

SCHEMATIC DIAGRAM OF DATA ACQUISITION SYSTEM

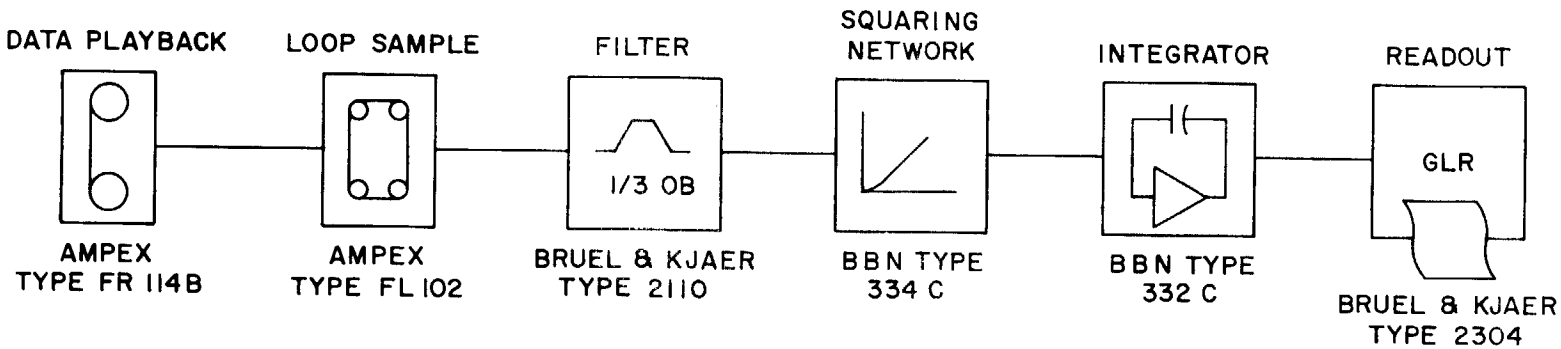

SCHEMATIC DIAGRAM OF SPECTRAL DATA REDUCTION SYSTEM

FIGURE 29 – INSTRUMENTATION USED TO TAKE SOUND MEASUREMENTS IN SATURN NOISE SURVEY

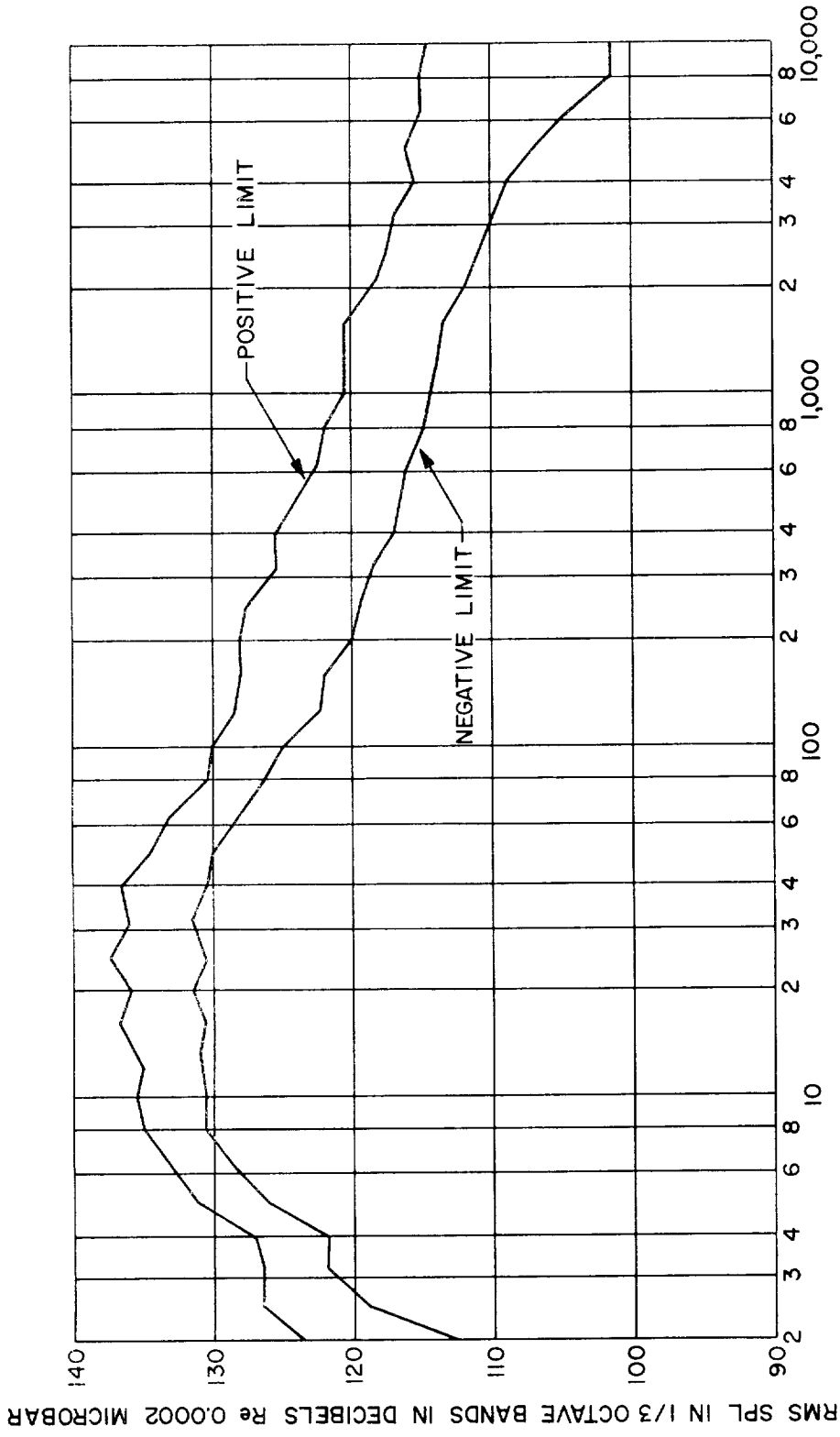

FIGURE 30 — RANGE OF DATA FOR ZERO° TO 30° MEASUREMENTS TAKEN DURING DURATION TESTS OF SATURN BOOSTER

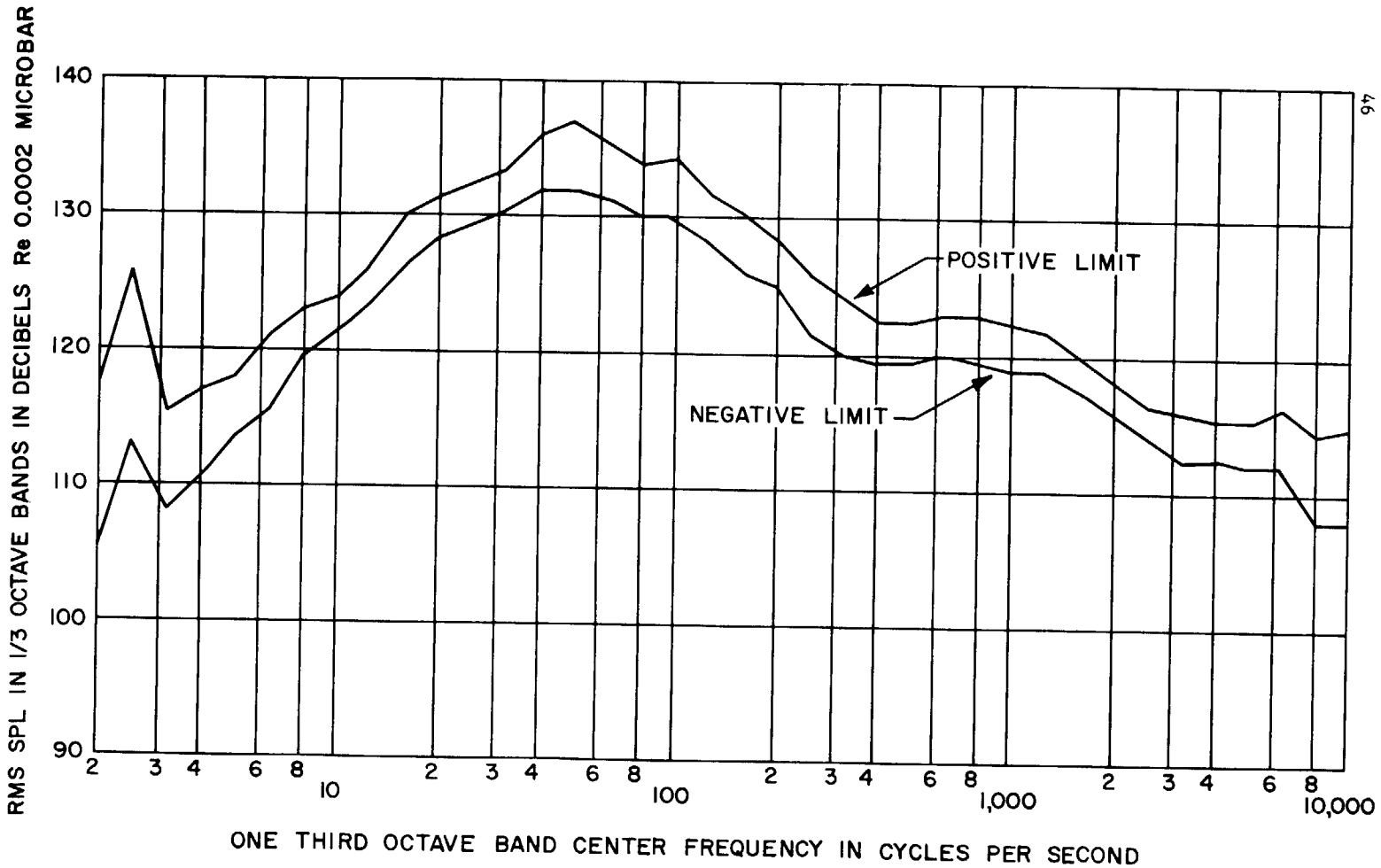

FIGURE 31 — RANGE OF DATA FOR 50° TO 70° MEASUREMENTS TAKEN DURING DURATION TESTS OF SATURN BOOSTER

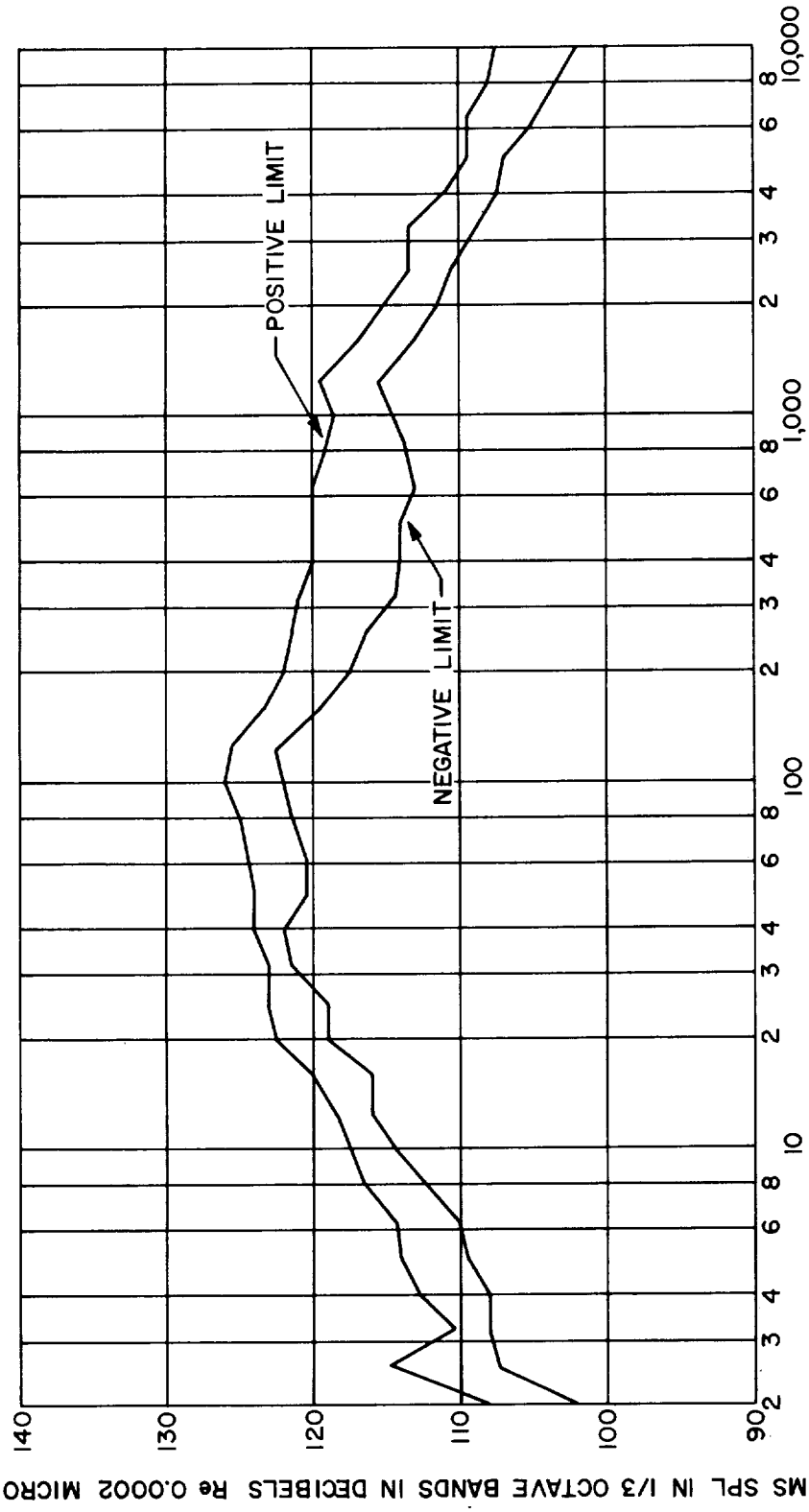

FIGURE 32 – RANGE OF DATA FOR 90° TO 150° MEASUREMENTS TAKEN DURING DURATION TESTS OF SATURN BOOSTER

REFERENCES

1. Anon.: Estimate of the Sound and Vibration Fields During Static Firing of a Saturn Vehicle and Analysis of the Damage problem. BBN Rpt 679, Bolt Beranek and Newman, Inc., January 1, 1960.

2. Anon.: Estimate of the Structural Response of a Saturn Vehicle in the Vicinity of the Engine Cluster During Launching. BBN Rpt 751, Bolt Beranek and Newman, Inc., June 28, 1960.

3. Anon.: Exterior Sound and Vibration Fields of a Saturn Vehicle During Static Firing and During Launching. BBN Final Rpt 764, Bolt Beranek and Newman, Inc., August 29, 1960.

4. Dorland, W.D.: Preliminary Estimation of Acoustic Conditions at the Saturn Launch Complex During the Initial Part of a Flight of the Saturn Booster. ABMA Rpt DTR-TR-2-60, January 20, 1960.

BIBLIOGRAPHY

1. Cole, J. N., et al: Noise Radiation from Fourteen Types of Rockets in the 1,000 to 130,000 Pounds Thrust Range. WADC Tech Rpt 57-354, December 1957.

2. Chobotov, V., and Powell, A.: On the Prediction of the Acoustic Environments from Rockets. Ramo-Wooldridge Rpt GM-TR-190, June 3, 1957.

3. Von Gierke, H. E.: Handbook of Noise Control (Chapter 33). McGraw-Hill Book Company, 1957.

4. Franken, P. A: Noise Reduction (Chapter 24). McGraw-Hill Book Company, 1960.

5. Honey, F. J.: Special Data Reduction Equipment: Amplitude Distribution Analyzer. Memo 20-190, Jet Propulsion Laboratory, July 16, 1959.

NASA TN D-611
National Aeronautics and Space Administration.
FAR-FIELD NOISE CHARACTERISTICS OF SATURN STATIC TESTS. Wade D. Dorland. August 1961. 48p. OTS price, $1.25.
(NASA TECHNICAL NOTE D-611)

Results of a far-field survey to determine the characteristics of the noise generated by Saturn static firing tests are presented and evaluated. Tests were made with two engines, four engines, and eight engines; sound power values were found to be 0.56, 1.6, and 25 to 40 megawatts, respectively, with corresponding acoustic efficiencies of 0.04 percent, 0.06 percent, and 0.7 percent. Frequency spectra peaked between 10 cps and 100 cps, with a severe dip at 250 cps and a minor peak at 1000 cps. Data obtained were insufficient to separate the effects of impingement on the flame deflector and the dampening of the cooling water from the effects the clustering of jet exhausts had on peaked pressure spectra and low efficiency.

I. Dorland, Wade D.
II. NASA TN D-611

(Initial NASA distribution: 4, Aircraft safety and noise; 23, Launching facilities and operations; 39, Propulsion systems, liquid-fuel rockets; 45, Research and development facilities; 51, Stresses and loads; 52, Structures; 53, Vehicle performance.)

NASA

NASA TN D-611
National Aeronautics and Space Administration.
FAR-FIELD NOISE CHARACTERISTICS OF SATURN STATIC TESTS. Wade D. Dorland. August 1961. 48p. OTS price, $1.25.
(NASA TECHNICAL NOTE D-611)

Results of a far-field survey to determine the characteristics of the noise generated by Saturn static firing tests are presented and evaluated. Tests were made with two engines, four engines, and eight engines; sound power values were found to be 0.56, 1.6, and 25 to 40 megawatts, respectively, with corresponding acoustic efficiencies of 0.04 percent, 0.06 percent, and 0.7 percent. Frequency spectra peaked between 10 cps and 100 cps, with a severe dip at 250 cps and a minor peak at 1000 cps. Data obtained were insufficient to separate the effects of impingement on the flame deflector and the dampening of the cooling water from the effects the clustering of jet exhausts had on peaked pressure spectra and low efficiency.

I. Dorland, Wade D.
II. NASA TN D-611

(Initial NASA distribution: 4, Aircraft safety and noise; 23, Launching facilities and operations; 39, Propulsion systems, liquid-fuel rockets; 45, Research and development facilities; 51, Stresses and loads; 52, Structures; 53, Vehicle performance.)

NASA

NASA TN D-611
National Aeronautics and Space Administration.
FAR-FIELD NOISE CHARACTERISTICS OF SATURN STATIC TESTS. Wade D. Dorland. August 1961. 48p. OTS price, $1.25.
(NASA TECHNICAL NOTE D-611)

Results of a far-field survey to determine the characteristics of the noise generated by Saturn static firing tests are presented and evaluated. Tests were made with two engines, four engines, and eight engines; sound power values were found to be 0.56, 1.6, and 25 to 40 megawatts, respectively, with corresponding acoustic efficiencies of 0.04 percent, 0.06 percent, and 0.7 percent. Frequency spectra peaked between 10 cps and 100 cps, with a severe dip at 250 cps and a minor peak at 1000 cps. Data obtained were insufficient to separate the effects of impingement on the flame deflector and the dampening of the cooling water from the effects the clustering of jet exhausts had on peaked pressure spectra and low efficiency.

I. Dorland, Wade D.
II. NASA TN D-611

(Initial NASA distribution: 4, Aircraft safety and noise; 23, Launching facilities and operations; 39, Propulsion systems, liquid-fuel rockets; 45, Research and development facilities; 51, Stresses and loads; 52, Structures; 53, Vehicle performance.)

NASA

NASA TN D-611
National Aeronautics and Space Administration.
FAR-FIELD NOISE CHARACTERISTICS OF SATURN STATIC TESTS. Wade D. Dorland. August 1961. 48p. OTS price, $1.25.
(NASA TECHNICAL NOTE D-611)

Results of a far-field survey to determine the characteristics of the noise generated by Saturn static firing tests are presented and evaluated. Tests were made with two engines, four engines, and eight engines; sound power values were found to be 0.56, 1.6, and 25 to 40 megawatts, respectively, with corresponding acoustic efficiencies of 0.04 percent, 0.06 percent, and 0.7 percent. Frequency spectra peaked between 10 cps and 100 cps, with a severe dip at 250 cps and a minor peak at 1000 cps. Data obtained were insufficient to separate the effects of impingement on the flame deflector and the dampening of the cooling water from the effects the clustering of jet exhausts had on peaked pressure spectra and low efficiency.

I. Dorland, Wade D.
II. NASA TN D-611

(Initial NASA distribution: 4, Aircraft safety and noise; 23, Launching facilities and operations; 39, Propulsion systems, liquid-fuel rockets; 45, Research and development facilities; 51, Stresses and loads; 52, Structures; 53, Vehicle performance.)

NASA